J. Appl. Comput. Mech., 4(4) (2018) 331-351
DOI: 10.22055/JACM.2018.24851.1214

ISSN: 2383-4536
jacm.scu.ac.ir

Shahid Chamran University of Ahvaz

Journal of Applied and Computational Mechanics

Research Article

Evaluation of the Best New Cross-ply Laminated Plate Theories through the Axiomatic/Asymptotic Approach

S. Candiotti[1], J. L. Mantari[1,2]

[1] Faculty of Mechanical Engineering, Universidad de Ingeniería y Tecnología (UTEC), Medrano Silva 165, Barranco, Lima, Perú

[2] University of New Mexico, Department of Mechanical Engineering, Albuquerque, New Mexico, U.S.A.

Received January 29 2018; Revised March 06 2018; Accepted for publication March 16 2018.
Corresponding author: J.L. Mantari, jmantari@utec.edu.pe

Abstract. This paper presents Best Theory Diagrams (BTDs) constructed from various non-polynomial theories for the static analysis of thick and thin symmetric and asymmetric cross-ply laminated plates. The BTD is a curve that provides the minimum number of unknown variables necessary for a fixed error or vice versa. The plate theories that belong to the BTD have been obtained by means of the Axiomatic/Asymptotic Method (AAM). The different plate theories reported are implemented by using the Carrera Unified Formulation (CUF). Navier-type solutions have been obtained for the case of simply- supported plates loaded by a bisinuisoidal transverse pressure with different length-to-thickness ratios. The BTDs built from non-polynomials functions are compared with BTDs using Maclaurin expansion. The results suggest that the plate models obtained from the BTD using non-polynomial terms can improve the accuracy obtained from Maclaurin expansions for a given number of unknown variables of the displacement field.

Keywords: Shear deformation; Best plate theory; Axiomatic–Asymptotic; Refined theories; Analytical modeling.

1. Introduction

Structural applications of laminated composite materials include different fields such as mechanical, civil, naval and aeronautic equipment. In such critical applications, accurate structural analysis is mandatory. The most accurate results of the mechanical response of a structure are obtained by solving 3D elasticity equations at the expense of high computational costs. To mitigate this effect, many axiomatic models have been developed based on different hypotheses typically by simplifying the 3D problem into a 2D one. The Classical laminated plate theory (CLPT) is based on the Kirchhoff-Love [1-2] hypothesis; as it is known, this theory offers good results for thin plates and in the cases where the shear stresses can be neglected. Furthermore, thick plates cannot be correctly analyzed and one of the primary concerns regarding laminate plates is the interlaminar failure due to shear stress. Addressing these concerns, the First Order Shear Deformation Laminate Theory (FSDLT) was developed based on the Reissner [3] and Mindlin [4] theories. However, FSDLT requires a correction factor, which is problem-dependent, to ensure the correct quantification of shear strain energy. Considering these limitations and in order to study the structural problems of higher complexity, the Higher Order Shear Deformation Laminate Theories (HSDLTs) were developed. HSDLT makes it possible to define the displacement field in polynomial or non-polynomial power series expansion of the thickness coordinate of any desired order. An important class of HSDLT is the Third Order Shear Laminate Theories, initially developed by Vlasov [5], Jemielita [6] and Schmidt [7] a review of which can be found in Ref. [8]. Non-polynomial HSDLT includes the use of trigonometric functions and are called trigonometric shear deformation plate theories (TSDPTs). Remarkable examples of TSDPTs and other non-polynomial functions include the works by Levy [9], Stein [10], Shimpi and Ghugal [11], Touratier [12], Soldatos [13], Ferreira [14], Karama et al. [15], Akavci [16], Mantari [17-18], Thai et al [19], Zenkour [20], Grover et al. [21], Sarangan and Singh [22] and Mahi et al. [23].

The present work is based on the Carrera Unified Formulation (CUF) introduced by Carrera [24]. The CUF allows defining the displacement and stress fields as an arbitrary expansion of the thickness coordinate of any desired order. The equilibrium equations can be written according to few fundamental nuclei whose form does not depend on either the expansion order or the choices made for the base functions. Extensive literature on CUF can be found in Refs. [25-28].

In this context, since some structural problems require the use of advanced plate theories and in others a low order theory can be sufficient, the CUF can be used as a way to analyze the best theory suitable for each problem. This procedure, introduced as the Axiomatic/Asymptotic Method (AAM) by Carrera and Petrolo [28, 29], provides the means to obtain asymptotic-like results starting from a preliminary axiomatic hypotheses by evaluating the effectiveness of each higher-order term against a reference solution and those variables whose influence can be neglected are not retained. The error determined via the AAM can be represented in a graphical form, with the error percentage in the abscissa and the number of unknown variables of the displacement field on the ordinate. The best suitable structural models given a number of unknown variables serve as the Pareto front; this is denoted as the Best Theory Diagram (BTD). The guidelines to build a BTD have been shown by Carrera and Petrolo [28], and research concerning the AAM applied to different structure elements can be found in Refs. [30-43]. The application of non-polynomial displacement fields within the CUF framework has been explored by Neves et al. [44], Carrera [45, 46], Filippi et al. [47, 48], Mantari et al. [49] and Ramos et al. [50].

In this paper, a compact and generalized mathematical model of the displacement which includes trigonometric and exponential shear strain shape functions is used to obtain reduced models for multilayered composited plates of various thickness ratios and configurations. The AAM is used to develop the BTDs for each proposed non-polynomial model and hindsight solutions are compared against the Maclaurin expansion BTDs using a fourth order Layer Wise model as a reference solution.

2. Analytical modeling based on Carrera Unified Formulation

Plate geometry and notations are given in Fig. 1. According to Carrera [14], the displacement of a plate structure can be described as:

$$\mathbf{u}(x,y,z) = F_s(z).\,u_s(x,y) \qquad s = 1,2,\dots,N \tag{1}$$

$$\boldsymbol{\delta}\mathbf{u}(x,y,z) = F_\tau(z).\,\delta u_\tau(x,y) \qquad \tau = 1,2,\dots,N \tag{2}$$

where $\mathbf{u}$ is the displacement vector (u_x, u_y, u_z) and N is the number of expansion terms. The expansion functions F_τ and F_s can be defined on the overall thickness of the plate. According to Einstein's notation, the repeated subscripts τ and s indicate summation. In this paper, the two approaches used are the equivalent single layer (ESL) and the layer-wise (LW) whose schemes can be found in Fig. 2.

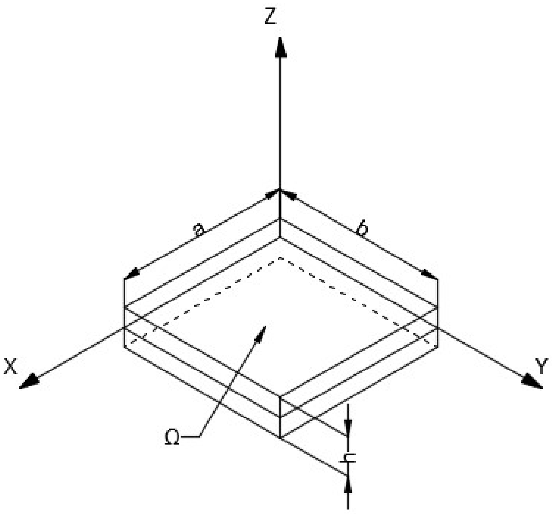

Fig. 1. Plate reference system and notations.

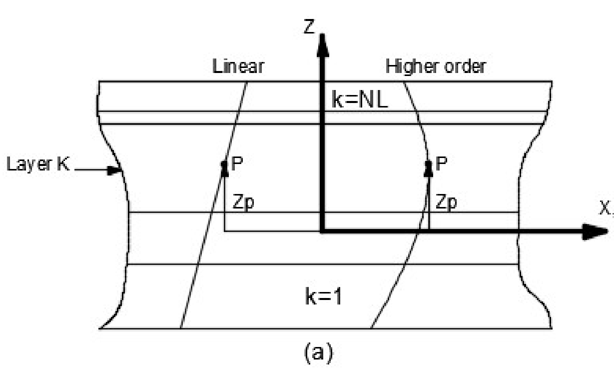

(a)

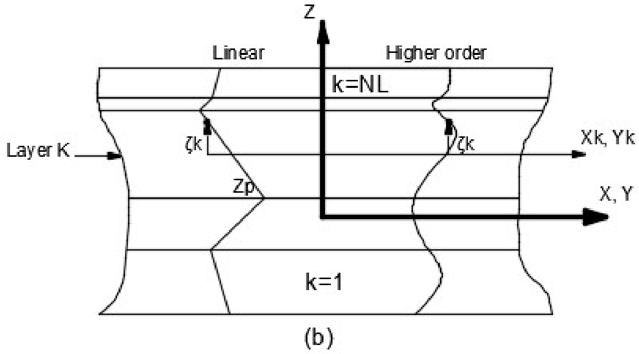

Fig. 2. Schemes of the theories used: (a) Equivalent single layer, and (b) Layer wise.

2.1 Equivalent single layer theory

The ESL approach represents the behavior of a multilayered plate as a single equivalent lamina. ESL models are indicated as EDN where N is the order of the expansion. An example of a displacement field using a fourth order Maclaurin expansion (ED4) is presented below:

$$u_x = u_{x1} + zu_{x2} + z^2u_{x3} + z^3u_{x4} + z^4u_{x5} \tag{3}$$

$$u_y = u_{y1} + zu_{y2} + z^2u_{y3} + z^3u_{y4} + z^4u_{y5} \tag{4}$$

$$u_z = u_{z1} + zu_{z2} + z^2u_{z3} + z^3u_{z4} + z^4u_{z5} \tag{5}$$

The Maclaurin expansion is considered as the polynomial expansion model (*pol*). As in Ref. [49], in addition to the polynomial expansion, this paper includes new non-polynomial expansions based on the sine (*sin*), tangent (*tan*) and exponential (*exp*) functions. (See Table 1).

Table 1. Expansion terms of the proposed theories.

Model	F_1	F_2	F_3	F_4	F_5
pol	1	z	z^2	z^3	z^4
sin	1	z	$\sin\left(\frac{z}{5h}\right)$	$\sin^2\left(\frac{z}{5h}\right)$	$\sin^3\left(\frac{z}{5h}\right)$
tan	1	z	$\tan\left(\frac{z}{5h}\right)$	$\tan^2\left(\frac{z}{5h}\right)$	$\tan^3\left(\frac{z}{5h}\right)$
exp	1	z	$ze^{\left(\frac{z}{5h}\right)^2}$	$z^2e^{\left(\frac{z}{5h}\right)^2}$	$z^3e^{\left(\frac{z}{5h}\right)^2}$

2.2 Layer-wise theory

Layer-wise models are denoted as LDN, where N is the order of the expansion, and they are built using the Legendre's polynomial expansions for each layer. The displacement field for an LD4 model can be described as:

$$u^k = F_t.u_t^k + F_b.u_b^k + F_r.u_r^k = F_\tau.u_\tau^k$$
$$\tau = t, b, r \qquad r = 2, 3, \dots, N \qquad k = 1, 2, \dots, N_L \tag{6a-b}$$

where N_L is the number of layers, *k* is a generic *k* layer and the subscripts *t* and *b* represent the top and bottom of a layer. Functions F_τ are derived from the Legendre's polynomials in the following manner:

$$F_t = \frac{P_0+P_1}{2}, \qquad F_b = \frac{P_0-P_1}{2}, \qquad F_r = P_r - P_{r-2}$$
$$P_0 = 1,\ P_1 = \zeta_k,\ P_2 = \frac{3\zeta_k^2-1}{2}, \tag{7a-h}$$
$$P_3 = \frac{5\zeta_k^3-3\zeta_k}{2}, \qquad P_4 = \frac{35\zeta_k^4-30\zeta_k^2+3}{8}$$

As the Legendre's polynomials are defined in the interval [-1,1], the following transformation is required:

$$\zeta_k = \frac{2}{z_{top}^k - z_{bot}^k} z - \frac{z_{top}^k + z_{bot}^k}{z_{top}^k - z_{bot}^k} \tag{8}$$

These polynomials satisfy the properties of orthogonaly and those of:

$$u_t^k = u_b^{k+1} \qquad k = 1, \dots, N_l - 1 \tag{9}$$

Finally, the LD4 displacement field used in this paper is presented as follows:

$$\begin{aligned} u_x^k &= F_t.u_{xt}^k + F_2.u_{x2}^k + F_3.u_{x3}^k + F_4.u_{x4}^k + F_b.u_{xb}^k \\ u_y^k &= F_t.u_{yt}^k + F_2.u_{y2}^k + F_3.u_{y3}^k + F_4.u_{y4}^k + F_b.u_{yb}^k \\ u_z^k &= F_t.u_{zt}^k + F_2.u_{z2}^k + F_3.u_{z3}^k + F_4.u_{z4}^k + F_b.u_{zb}^k \end{aligned} \tag{10a-c}$$

2.3. Elastic stress–strain relation

The stress (σ) and the strain (ε) are grouped as follows:

$$\boldsymbol{\sigma}_p^k = \left[\sigma_{xx}^k\ \sigma_{yy}^k\ \sigma_{xy}^k\right]^T, \qquad \boldsymbol{\sigma}_n^k = \left[\sigma_{xz}^k\ \sigma_{yz}^k\ \sigma_{zz}^k\right]^T,$$
$$\boldsymbol{\varepsilon}_p^k = \left[\varepsilon_{xx}^k\ \varepsilon_{yy}^k\ \gamma_{xy}^k\right]^T, \qquad \boldsymbol{\varepsilon}_n^k = \left[\gamma_{xz}^k\ \gamma_{yz}^k\ \varepsilon_{zz}^k\right]^T, \tag{11a-d}$$

The subscript "n" is related to the in-plane components, while "p" is related to the out-of-plane components. The strain – displacement relationships are given as:

$$\boldsymbol{\varepsilon}_p^k = D_p\mathbf{u}^k ,$$
$$\boldsymbol{\varepsilon}_n^k = D_n\mathbf{u}^k = \left(D_{np} + D_{nz}\right)\mathbf{u}^k$$
$$D_p = \begin{bmatrix} \frac{\partial}{\partial x} & 0 & 0 \\ 0 & \frac{\partial}{\partial y} & 0 \\ \frac{\partial}{\partial y} & \frac{\partial}{\partial x} & 0 \end{bmatrix}, \qquad D_{np} = \begin{bmatrix} 0 & 0 & \frac{\partial}{\partial x} \\ 0 & 0 & \frac{\partial}{\partial y} \\ 0 & 0 & 0 \end{bmatrix}, \qquad D_{nz} = \begin{bmatrix} \frac{\partial}{\partial z} & 0 & 0 \\ 0 & \frac{\partial}{\partial z} & 0 \\ 0 & 0 & \frac{\partial}{\partial z} \end{bmatrix} \tag{12a-c}$$

The stress – strain relationships corresponding to an orthotropic material can be expressed according to the Hooke law:

$$\boldsymbol{\sigma}^k = \mathbf{C}^k\boldsymbol{\varepsilon}^k$$
$$\begin{Bmatrix} \sigma_{xx}^k \\ \sigma_{yy}^k \\ \sigma_{xy}^k \\ \sigma_{yz}^k \\ \sigma_{xz}^k \\ \sigma_{zz}^k \end{Bmatrix} = \begin{bmatrix} C_{11}^k & C_{12}^k & 0 & 0 & 0 & C_{13}^k \\ C_{12}^k & C_{22}^k & 0 & 0 & 0 & C_{23}^k \\ 0 & 0 & C_{66}^k & 0 & 0 & 0 \\ 0 & 0 & 0 & C_{44}^k & 0 & 0 \\ 0 & 0 & 0 & 0 & C_{55}^k & 0 \\ C_{13}^k & C_{23}^k & 0 & 0 & 0 & C_{33}^k \end{bmatrix} \begin{Bmatrix} \varepsilon_{xx}^k \\ \varepsilon_{yy}^k \\ \gamma_{xy}^k \\ \gamma_{yz}^k \\ \gamma_{xz}^k \\ \varepsilon_{zz}^k \end{Bmatrix} \tag{13a-b}$$

and the stiffness coefficients C_{ij}^k in terms of the engineering constants are given below:

$$\begin{aligned} C_{11}^k &= \frac{1-v_{23}^k v_{32}^k}{E_2^k E_3^k \Delta^k} \\ C_{12}^k &= \frac{v_{21}^k + v_{31}^k v_{23}^k}{E_2^k E_3^k \Delta^k} = \frac{v_{12}^k + v_{32}^k v_{13}^k}{E_1^k E_3^k \Delta^k} \\ C_{13}^k &= \frac{v_{31}^k + v_{21}^k v_{32}^k}{E_2^k E_3^k \Delta^k} = \frac{v_{13}^k + v_{12}^k v_{23}^k}{E_1^k E_2^k \Delta^k} \\ C_{22}^k &= \frac{1-v_{13}^k v_{31}^k}{E_1^k E_3^k \Delta^k} \\ C_{23}^k &= \frac{v_{32}^k + v_{12}^k v_{31}^k}{E_1^k E_3^k \Delta^k} = \frac{v_{23}^k + v_{21}^k v_{13}^k}{E_1^k E_3^k \Delta^k} \\ C_{33}^k &= \frac{1-v_{12}^k v_{21}^k}{E_1^k E_2^k \Delta^k} \\ C_{44}^k &= G_{23}^k \\ C_{55}^k &= G_{31}^k \\ C_{66}^k &= G_{12}^k \\ \Delta^k &= \frac{1-v_{12}^k v_{21}^k - v_{23}^k v_{32}^k - v_{31}^k v_{12}^k - 2v_{21}^k v_{32}^k v_{13}^k}{E_1^k E_2^k E_3^k} \end{aligned} \tag{14a-m}$$

$$v_{21}^{k}=\frac{E_2^k v_{12}^k}{E_1^k}$$

$$v_{31}^{k}=\frac{E_3^k v_{13}^k}{E_1^k}$$

$$v_{32}^{k}=\frac{E_3^k v_{23}^k}{E_2^k}$$

Material stiffnesses coeficients $\mathrm{C}_{\mathrm{ij}}^{\mathrm{k}}$ are transformed from the material coordinate system to the problem coordinates via the following equations:

$$[\tilde{\mathbf{C}}^{\mathrm{k}}]=[\mathbf{T}^{\mathrm{k}}][\mathbf{C}^{\mathrm{k}}][\mathbf{T}^{\mathrm{k}}]^{T} \tag{15}$$

$$[\mathbf{T}^{\mathrm{k}}]=\begin{bmatrix} \cos^2\theta^{\mathrm{k}} & \sin^2\theta^{\mathrm{k}} & -\sin 2\theta^{\mathrm{k}} & 0 & 0 & 0\\ \sin^2\theta^{\mathrm{k}} & \cos^2\theta^{\mathrm{k}} & \sin 2\theta^{\mathrm{k}} & 0 & 0 & 0\\ \cos\theta^{\mathrm{k}}\sin\theta^{\mathrm{k}} & -\cos\theta^{\mathrm{k}}\sin\theta^{\mathrm{k}} & \cos^2\theta^{\mathrm{k}}-\sin^2\theta^{\mathrm{k}} & 0 & 0 & 0\\ 0 & 0 & 0 & \cos\theta^{\mathrm{k}} & \sin\theta^{\mathrm{k}} & 0\\ 0 & 0 & 0 & -\sin\theta^{\mathrm{k}} & \cos\theta^{\mathrm{k}} & 0\\ 0 & 0 & 0 & 0 & 0 & 1 \end{bmatrix} \tag{16}$$

And θ^k is the lamina´s angle oriented counterclockwise from the x-axis. For an orthotropic material, the stiffness coefficients can be grouped as follows:

$$\tilde{\mathbf{C}}_{\mathrm{pp}}^{\mathrm{k}}=\begin{bmatrix}\tilde{C}_{11}^{k} & \tilde{C}_{12}^{k} & 0\\ \tilde{C}_{12}^{k} & \tilde{C}_{22}^{k} & 0\\ 0 & 0 & \tilde{C}_{66}^{k}\end{bmatrix} \qquad \tilde{\mathbf{C}}_{\mathrm{pn}}^{\mathrm{k}}=\begin{bmatrix}0 & 0 & \tilde{C}_{13}^{k}\\ 0 & 0 & \tilde{C}_{23}^{k}\\ 0 & 0 & 0\end{bmatrix}$$

$$\tilde{\mathbf{C}}_{\mathrm{np}}^{\mathrm{k}}=\begin{bmatrix}0 & 0 & 0\\ 0 & 0 & 0\\ \tilde{C}_{13}^{k} & \tilde{C}_{23}^{k} & 0\end{bmatrix} \qquad \tilde{\mathbf{C}}_{\mathrm{nn}}^{\mathrm{k}}=\begin{bmatrix}\tilde{C}_{55}^{k} & 0 & 0\\ 0 & \tilde{C}_{44}^{k} & 0\\ 0 & 0 & \tilde{C}_{33}^{k}\end{bmatrix} \tag{17a-d}$$

The Hooke law can be defined in terms of the in-plane and out-of-plane terms:

$$\begin{aligned}\boldsymbol{\sigma}_{\mathrm{p}}^{\mathrm{k}}&=\left(\tilde{\mathbf{C}}_{\mathrm{pp}}^{\mathrm{k}}\boldsymbol{\varepsilon}_{\mathrm{p}}^{\mathrm{k}}+\tilde{\mathbf{C}}_{\mathrm{pn}}^{\mathrm{k}}\boldsymbol{\varepsilon}_{\mathrm{n}}^{\mathrm{k}}\right)\\ \boldsymbol{\sigma}_{\mathrm{n}}^{\mathrm{k}}&=\left(\tilde{\mathbf{C}}_{\mathrm{np}}^{\mathrm{k}}\boldsymbol{\varepsilon}_{\mathrm{p}}^{\mathrm{k}}+\tilde{\mathbf{C}}_{\mathrm{nn}}^{\mathrm{k}}\boldsymbol{\varepsilon}_{\mathrm{n}}^{\mathrm{k}}\right)\end{aligned} \tag{18a-b}$$

2.4. Governing Equations

The plate static analysis considers the equilibrium via the principle of virtual displacement (PVD) as follows:

$$\delta \mathrm{L}_{\mathrm{int}}=\delta \mathrm{L}_{\mathrm{ext}} \tag{19}$$

where $\delta\mathrm{L}_{\mathrm{int}}$ is the virtual variation of the internal work and $\delta\mathrm{L}_{\mathrm{ext}}$ is the virtual variation of the external work. The PVD can be written as:

$$\sum_{k=1}^{N_l}\int_{z}\int_{\Omega}\left(\delta\boldsymbol{\varepsilon}_{\mathrm{p}}^{k^T}\boldsymbol{\sigma}_{\mathrm{p}}^{\mathrm{k}}+\delta\boldsymbol{\varepsilon}_{\mathrm{n}}^{k^T}\boldsymbol{\sigma}_{\mathrm{n}}^{k}\right)\mathrm{d}\Omega\mathrm{d}z=\sum_{k=1}^{N_l}\delta \mathrm{L}_{\mathrm{ext}}^{k} \tag{20}$$

Using Eqs. (13a-b), (19a-b), Eq. (20) becomes:

$$\int_{\Omega_{\mathrm{k}}}\int_{z}\{(\mathbf{D}_{\mathrm{p}}\delta\mathbf{u}^{\mathrm{k}})^{\mathrm{T}}[\tilde{\mathbf{C}}_{\mathrm{pp}}^{\mathrm{k}}\mathbf{D}_{\mathrm{p}}+\tilde{\mathbf{C}}_{\mathrm{pn}}^{\mathrm{k}}(\mathbf{D}_{\mathrm{np}}+\mathbf{D}_{\mathrm{nz}})]\mathbf{u}^{\mathrm{k}}+[(\mathbf{D}_{\mathrm{np}}+\mathbf{D}_{\mathrm{nz}})\delta\mathbf{u}^{\mathrm{k}}]^{\mathrm{T}}[\tilde{\mathbf{C}}_{\mathrm{np}}^{\mathrm{k}}\mathbf{D}_{\mathrm{p}}+\tilde{\mathbf{C}}_{\mathrm{nn}}^{\mathrm{k}}(\mathbf{D}_{\mathrm{np}}+\mathbf{D}_{\mathrm{nz}})]\mathbf{u}^{\mathrm{k}}\}\mathrm{d}\Omega_{\mathrm{k}}\mathrm{d}z=\delta\mathrm{L}_{\mathrm{e}}^{\mathrm{k}} \tag{21}$$

By replacing Eqs. (1a-b) in Eq. (21), the following expression can be obtained.

$$\begin{aligned}&\int_{\Omega_{\mathrm{k}}}\int_{z}\{(\mathbf{D}_{\mathrm{p}}\delta\mathbf{u}_{\tau}^{\mathrm{k}})^{T}(\mathrm{F}_{\tau}\mathrm{F}_{\mathrm{s}}\tilde{\mathbf{C}}_{\mathrm{pp}}^{\mathrm{k}}\mathbf{D}_{\mathrm{p}}\mathbf{u}_{\mathrm{s}}^{\mathrm{k}}+\mathrm{F}_{\tau}\mathrm{F}_{\mathrm{s}}\tilde{\mathbf{C}}_{\mathrm{pn}}^{\mathrm{k}}\mathbf{D}_{\mathrm{np}}\mathbf{u}_{\mathrm{s}}^{\mathrm{k}}+\mathrm{F}_{\tau}\mathrm{F}_{\mathrm{s},z}\tilde{\mathbf{C}}_{\mathrm{pn}}^{\mathrm{k}}\mathbf{u}_{\mathrm{s}}^{\mathrm{k}})+(\mathbf{D}_{\mathrm{np}}\delta\mathbf{u}_{\tau}^{\mathrm{k}})^{T}[\mathrm{F}_{\tau}\mathrm{F}_{\mathrm{s}}\tilde{\mathbf{C}}_{\mathrm{np}}^{\mathrm{k}}\mathbf{D}_{\mathrm{p}}\mathbf{u}_{\mathrm{s}}^{\mathrm{k}}+\mathrm{F}_{\tau}\mathrm{F}_{\mathrm{s}}\tilde{\mathbf{C}}_{\mathrm{nn}}^{\mathrm{k}}\mathbf{D}_{\mathrm{np}}\mathbf{u}_{\mathrm{s}}^{\mathrm{k}}+\mathrm{F}_{\tau}\mathrm{F}_{\mathrm{s},z}\tilde{\mathbf{C}}_{\mathrm{nn}}^{\mathrm{k}}\mathbf{u}_{\mathrm{s}}^{\mathrm{k}}]\\ &+(\delta\mathbf{u}_{\tau}^{\mathrm{k}})^{\mathrm{T}}[\mathrm{F}_{\tau,z}\mathrm{F}_{\mathrm{s}}\tilde{\mathbf{C}}_{\mathrm{np}}^{\mathrm{k}}\mathbf{D}_{\mathrm{p}}\mathbf{u}_{\mathrm{s}}^{\mathrm{k}}+\mathrm{F}_{\tau,z}\mathrm{F}_{\mathrm{s}}\tilde{\mathbf{C}}_{\mathrm{nn}}\mathbf{D}_{\mathrm{np}}\mathbf{u}_{\mathrm{s}}^{\mathrm{k}}+\mathrm{F}_{\tau,z}\mathrm{F}_{\mathrm{s},z}\tilde{\mathbf{C}}_{\mathrm{nn}}^{\mathrm{k}}\mathbf{u}_{\mathrm{s}}^{\mathrm{k}}]\}\mathrm{d}\Omega_{\mathrm{k}}\mathrm{d}z=\delta\mathrm{L}_{\mathrm{e}}^{\mathrm{k}}\end{aligned} \tag{22}$$

Applying integration by parts in the following cases:

$$\int_{\psi}(\mathrm{D}_{\varsigma}\delta\mathrm{a}_{\tau}^{\mathrm{k}})^{\mathrm{T}}\mathrm{a}_{\mathrm{s}}^{\mathrm{k}}\mathrm{d}\psi=-\int_{\psi}\delta\mathrm{a}_{\tau}^{\mathrm{k}^{\mathrm{T}}}(\mathrm{D}_{\varsigma}^{\mathrm{T}}\mathrm{a}_{\mathrm{s}}^{\mathrm{k}})\mathrm{d}\psi+\int_{\Gamma}\delta\mathrm{a}_{\tau}^{\mathrm{k}^{\mathrm{T}}}(\mathrm{I}_{\varsigma}^{\mathrm{T}}\mathrm{a}_{\mathrm{s}}^{\mathrm{k}})\mathrm{d}\Gamma \tag{23}$$

where $\varsigma=\mathrm{p},\mathrm{np}$. Applying the integration by parts as in Eq. (23), Eq. (22) becomes:

$$\int_{\Omega_{\mathrm{k}}}\int_{z}\delta\mathbf{u}_{\tau}^{\mathrm{k}^T}\mathbf{K}_{\mathrm{d}}^{\mathrm{k\tau s}}\mathbf{u}_{\mathrm{s}}^{\mathrm{k}}\mathrm{d}z\mathrm{d}\Omega+\int_{\Gamma}\delta\mathbf{u}_{\tau}^{\mathrm{k}^T}\boldsymbol{\Pi}_{\mathrm{d}}^{\mathrm{k\tau s}}\mathbf{u}_{\mathrm{s}}^{\mathrm{k}}\mathrm{d}\Pi=\delta\mathbf{L}_{\mathrm{e}}^{\mathrm{k}} \tag{24}$$

where:

$$\mathbf{K}_{d}^{k\tau s} = -\mathbf{D}_{p}^{T}\left(F_\tau F_s \tilde{\mathbf{C}}_{pp}^{k}\mathbf{D}_{p} + F_\tau F_s \tilde{\mathbf{C}}_{np}^{k}\mathbf{D}_{np}^{k} + F_\tau F_{s,z}\tilde{\mathbf{C}}_{pn}^{k}\right) - \mathbf{D}_{np}^{T}\left(F_\tau F_s \tilde{\mathbf{C}}_{np}^{k} D_p + F_\tau F_s \tilde{\mathbf{C}}_{nn}^{k}\mathbf{D}_{np} + F_\tau F_{s,z}\tilde{\mathbf{C}}_{nn}^{k}\right) + F_{\tau,z}F_s\tilde{\mathbf{C}}_{np}^{k}\mathbf{D}_{p} + F_{\tau,z}F_s\tilde{\mathbf{C}}_{nn}^{k}\mathbf{D}_{np} + F_{\tau,z}F_{s,z}\tilde{\mathbf{C}}_{nn}^{k}) \tag{25}$$

$$\mathbf{\Pi}_{d}^{k\tau s} = \mathbf{I}_{p}^{k\,T}\left(F_\tau F_s \tilde{\mathbf{C}}_{np}^{k}\mathbf{D}_{p} + F_\tau F_s \tilde{\mathbf{C}}_{nn}^{k}\mathbf{D}_{np} + F_\tau F_{s,z}\tilde{\mathbf{C}}_{pn}^{k}\right) + \mathbf{I}_{np}^{k\,T}(F_\tau F_s \tilde{\mathbf{C}}_{np}^{k}\mathbf{D}_{p} + F_\tau F_s \tilde{\mathbf{C}}_{nn}^{k}\mathbf{D}_{np} + F_\tau F_{s,z}\tilde{\mathbf{C}}_{nn}^{k}) \tag{26}$$

The external work is expressed as:

$$\delta\mathbf{L}_{e}^{k} = \int_{\Omega} \delta\mathbf{u}_{\tau}^{k^T}\mathbf{P}_{\tau}^{k}d\Omega \tag{27}$$

$$\mathbf{P}_{\tau}^{k} = \left[0\ 0\ \bar{F}_\tau q_{z(x,y)}\right]^T \qquad \bar{F}_\tau = F_{\tau(z=h/2)} \tag{28}$$

$$\mathbf{I}_{p}^{k} = \begin{bmatrix}1 & 0 & 0\\ 0 & 1 & 0\\ 1 & 1 & 0\end{bmatrix} \tag{29}$$

$$\mathbf{uI}_{np}^{k} = \begin{bmatrix}0 & 0 & 1\\ 0 & 0 & 1\\ 0 & 0 & 0\end{bmatrix} \tag{30}$$

Finally, the governing equations are:

$$(\delta u_\tau^k)^T\!:\ \mathbf{K}_{d}^{k\tau s}\mathbf{u}_{s}^{k} = \mathbf{P}_{s}^{k} \tag{31}$$

With boundary condition stated as:

$$\mathbf{\Pi}_{d}^{k\tau s}\mathbf{u}_{s} = \mathbf{\Pi}_{d}^{k\tau s}\bar{\mathbf{u}}_{s} \tag{32}$$

$\mathbf{P}_{\tau}^{k}$ is the external load. The fundamental nucleus, $\mathbf{K}_{d}^{k\tau s}$, is expanded through the indexes, τ and s. The superscript *k* denotes the assembling on the number of layers.

2.5. Analytical solution

Navier-type closed-form solutions have been obtained for the case of simply-supported plates. The displacement variable and the transverse distributed load for an LW model can be expressed in the following Fourier series:

$$\begin{aligned}
u_{x\tau}^{k} &= \textstyle\sum_{m,n}(U_{xs}^{k})\cos(\alpha x)\sin(\beta y) && 0 \le x \le a;\ 0 \le y \le b\\
u_{y\tau}^{k} &= \textstyle\sum_{m,n}(U_{ys}^{k})\sin(\alpha x)\cos(\beta y) && 0 \le x \le a;\ 0 \le y \le b\\
u_{z\tau}^{k} &= \textstyle\sum_{m,n}(U_{zs}^{k})\sin(\alpha x)\sin(\beta y) && 0 \le x \le a;\ 0 \le y \le b\\
q_{z} &= \textstyle\sum_{m,n}(Q_{z})\sin(\alpha x)\sin(\beta y) && 0 \le x \le a;\ 0 \le y \le b\\
&\alpha = \frac{m\pi}{a},\ \beta = \frac{n\pi}{b}
\end{aligned} \tag{33a-f}$$

where $U_{x\tau}^{k}$, $U_{y\tau}^{k}$, $U_{z\tau}^{k}$ and Q_z are the amplitudes, m and n are the number of waves (which can range from 0 to ∞) and a and b are the plate lengths in the x and y directions, respectively. For the ESL model, the same solution can be applied without the subscript k. Consequentely, the governing equation (31) can be expresed as:

$$\begin{bmatrix}\bar{K}_{11}^{k\tau s} & \bar{K}_{12}^{k\tau s} & \bar{K}_{13}^{k\tau s}\\ \bar{K}_{21}^{k\tau s} & \bar{K}_{22}^{k\tau s} & \bar{K}_{23}^{k\tau s}\\ \bar{K}_{31}^{k\tau s} & \bar{K}_{32}^{k\tau s} & \bar{K}_{33}^{k\tau s}\end{bmatrix}\begin{bmatrix}U_{xs}^{k}\\ U_{ys}^{k}\\ U_{zs}^{k}\end{bmatrix} = \begin{bmatrix}0\\ 0\\ \bar{F}_\tau Q_z\end{bmatrix} \tag{34}$$

$$\begin{aligned}
\bar{K}_{11}^{k\tau s} &= \int_z \left(\tilde{C}_{55}^{k}F_{\tau,z}F_{s,z} + \alpha^2\tilde{C}_{11}^{k}F_\tau F_s + \beta^2\tilde{C}_{66}^{k}F_\tau F_s\right)dz\\
\bar{K}_{12}^{k\tau s} &= \int_z \left(\alpha\beta\tilde{C}_{12}^{k}F_\tau F_s + \alpha\beta\tilde{C}_{66}^{k}F_\tau F_s\right)dz\\
\bar{K}_{13}^{k\tau s} &= \int_z \left(-\alpha\tilde{C}_{13}^{k}F_\tau F_{s,z} + \alpha\tilde{C}_{55}^{k}F_{\tau,z}F_s\right)dz\\
\bar{K}_{21}^{k\tau s} &= \int_z \left(\alpha\beta\tilde{C}_{12}^{k}F_\tau F_s + \alpha\beta\tilde{C}_{66}^{k}F_\tau F_s\right)dz
\end{aligned} \tag{35a-i}$$

$$\overline{K}_{22}^{k\tau s} = \int_{z} \left(\tilde{C}_{55}^{k} F_{\tau,z} F_{s,z} + \alpha^2 \tilde{C}_{66}^{k} F_{\tau} F_{s} + \beta^2 \tilde{C}_{22}^{k} F_{\tau} F_{s}\right) dz$$

$$\overline{K}_{23}^{k\tau s} = \int_{z} \left(-\beta \tilde{C}_{23}^{k} F_{\tau} F_{s,z} + \beta \tilde{C}_{44}^{k} F_{\tau,z} F_{s}\right) dz$$

$$\overline{K}_{31}^{k\tau s} = \int_{z} \left(\alpha \tilde{C}_{55}^{k} F_{\tau} F_{s,z} - \alpha \tilde{C}_{13}^{k} F_{\tau,z} F_{s}\right) dz$$

$$\overline{K}_{32}^{k\tau s} = \int_{z} \left(\beta \tilde{C}_{44}^{k} F_{\tau} F_{s,z} - \beta \tilde{C}_{23}^{k} F_{\tau,z} F_{s}\right) dz$$

$$\overline{K}_{33}^{k\tau s} = \int_{z} \left(\tilde{C}_{33}^{k} F_{\tau,z} F_{s,z} + \alpha^2 \tilde{C}_{55}^{k} F_{\tau} F_{s} + \beta^2 \tilde{C}_{44}^{k} F_{\tau} F_{s}\right) dz$$

3. Axiomatic/Asymptotic Method

Refined plate theories offer significant advantages in terms of analysis accuracy at the expense of higher computational costs because of the presence of a large number of displacement variables. Previous works [28-43] have highlighted that not all terms of the expansion have the same influence and that it is possible to obtain reduced models, which show the same or even better accuracy than the full model. As reported in Ref. [28], the effectiveness of each term has been investigated as follows:
1. The problem inputs are fixed (i.e. geometry, boundary conditions, loadings, materials).
2. A set of output unknown variables is chosen (e.g. maximum displacement, stress/displacement component at a given point).
3. The CUF is used to generate the governing equations for the considered theories.
4. A reference solution is used to establish the accuracy (in this paper, a full LD4 theory is used as the reference result).
5. A theory or model is chosen, that is, the terms that have to be considered in the expansion of u_x, u_y and u_z are established.
6. The accuracy of each theory or model is numerically established by measuring the error produced with respect to the reference solution.
7. The most suitable kinematic model for a given structural problem is then obtained by discarding the non-effective displacement unknown variables.

A graphic notation has been introduced to improve the readability of the results. This notation consists of a table with three rows, and a number of columns equal to the number of the displacement variable used in the expansion. The notation adopted for active and inactive terms is given in Table 2. As an example, the representation of an ED4 full model and a reduced model, where the displacement variable u_{y2} is deactivated, is presented in Table 3.

Table 2. Example of model representation.

Active term	Inactive terms
▲	Δ

Table 3. Symbols to indicate the status of a displacement variable.

Full model representation

▲	▲	▲	▲	▲
▲	▲	▲	▲	▲
▲	▲	▲	▲	▲

Reduced model representation

▲	▲	▲	▲	▲
▲	Δ	▲	▲	▲
▲	▲	▲	▲	▲

The BTD can be built by evaluating the accuracy of all the models given by combining all the terms of an expansion. Therefore, for each expansion of this paper, 2^{15} models have been evaluated. The BTD is made of all those models that, for a given number of terms, provide the best accuracy; or, conversely, for a given accuracy, the BTD model requires the least number of terms.

4. Results and discussion

Axiomatic/asymptotic analysis results are reported for laminated simply-supported square plates. The load is a bisinusoidal transverse pressure applied at the top surface of the plate:

$$p = \bar{p}_z \cdot \sin\left(\frac{m\pi x}{a}\right) \sin\left(\frac{n\pi y}{b}\right) \tag{36}$$

Here the amplitude $\bar{p}_z$ is equal to 1 KPa. Throughout the analysis, the number of waves *m* and *n* were equal to *m* = *n* = 1. Geometrical notations and the reference system are given in Fig. 1. Reduced models were developed to evaluate $\bar{\sigma}_{xx}$ and $\bar{\sigma}_{xz}$ stresses in all the studied cases. The results were computed at $(\frac{a}{2}, \frac{b}{2}, z)$ with $-\frac{h}{2} \leq z \leq \frac{h}{2}$, where h is the total thickness of the plate. The material properties were $E_L/E_T = 25, G_{LT}/E_T = 0.5, G_{TT}/E_T = 0.2$, and $v_{LT} = v_{TT} = 0.25$. The evaluated cases were two symmetric laminated plates with ply sequences of 0°/90°/0° and 0°/90°/90°/0°, and an asymmetric laminated plate with a ply sequence of 0°/90°; each layer had the same thickness. For reference, an LD4 model was employed. Moreover, BTDs from the functions introduced by Mantari et al. [49] and Candiotti et al. [52] were presented for comparison, which were denoted as *sin**, *hyp** and *exp** models. In all cases, the length-to-thickness ratios were 4 and 20. To ensure no transverse shear stress discontinuity, the shear stress was computed by means of the following equation:

$$\sigma_{xz} = -\int \left(\frac{\partial \sigma_{xx}}{\partial x} + \frac{\partial \sigma_{xy}}{\partial y}\right)dz$$
$$\sigma_{yz} = -\int \left(\frac{\partial \sigma_{xy}}{\partial x} + \frac{\partial \sigma_{yy}}{\partial y} +\right)dz \tag{37a-b}$$

A multi-points error evaluation along the thickness proposed by Carrera et al. [39] was implemented. The error of the new models with respect to a reference solution was evaluated through the following formula:

$$e = 100\frac{\sum_{i=1}^{N_p}\left|Q^i - Q^i_{ref}\right|}{maxQ_{ref} \cdot N_p} \tag{38}$$

where Q can be a stress/displacement component and N_p is the number of points along the thickness on which the entity Q is computed.

4.1 Symmetric laminated plates

Two symmetric cross-ply square plates were considered for this analysis, with three layers [0°/90°/0°] and four layers [0°/90°/90°/0°]. The normalization of deflection and stresses for the model assessment were defined in concordance with the following equations:

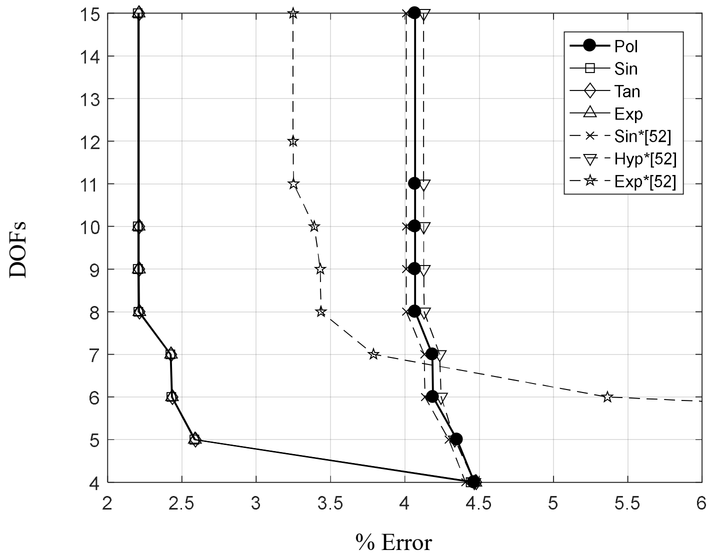

(a) $^{a}/_{h} = 4$

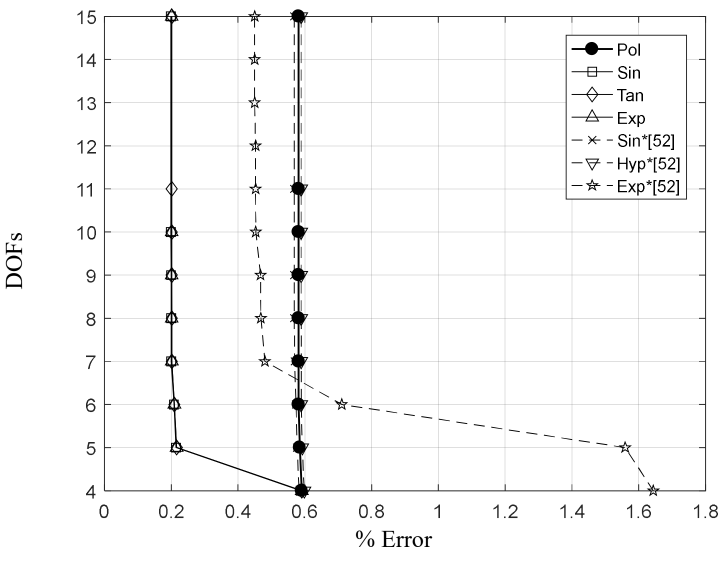

(b) $^{a}/_{h} = 20$

Fig. 3. Comparison between BTDs of polynomial and non-polynomial ED4 models build by the AAM for σ_{xx} stress in three layers laminated plate, (a) $^{a}/_{h}$=4, (b) $^{a}/_{h}$=20.

For three layers [0°/90°/0°]:

$$\overline{w}=\frac{100E_2h^3}{q_oa^4}w_o\left(\frac{a}{2},\frac{b}{2},0\right),\ \overline{\sigma}_{xx}=\frac{h^2}{q_oa^2}\sigma_{xx}\left(\frac{a}{2},\frac{b}{2},-\frac{h}{2}\right),$$
$$\overline{\sigma}_{yy}=\frac{h^2}{q_oa^2}\sigma_{yy}\left(\frac{a}{2},\frac{b}{2},-\frac{h}{6}\right),\overline{\tau}_{xy}=\frac{h^2}{q_oa^2}\tau_{xy}\left(0,0,-\frac{h}{2}\right), \tag{39a-f}$$
$$\overline{\tau}_{xz}=\frac{h}{q_oa}\tau_{xz}\left(0,\frac{b}{2},0\right),\quad \overline{\tau}_{yz}=\frac{h}{q_oa}\tau_{yz}\left(\frac{a}{2},0,0\right)$$

For four layers [0°/90°90°0°]:

$$\overline{w}=\frac{100E_2h^3}{q_oa^4}w_o\left(\frac{a}{2},\frac{b}{2},0\right),\ \overline{\sigma}_{xx}=\frac{h^2}{q_oa^2}\sigma_{xx}\left(\frac{a}{2},\frac{b}{2},\frac{h}{2}\right),$$
$$\overline{\sigma}_{yy}=\frac{h^2}{q_oa^2}\sigma_{yy}\left(\frac{a}{2},\frac{b}{2},\frac{h}{4}\right),\quad \overline{\tau}_{xy}=\frac{h^2}{q_oa^2}\tau_{xy}\left(0,0,\frac{h}{2}\right), \tag{40a-f}$$
$$\overline{\tau}_{xz}=\frac{h}{q_oa}\tau_{xz}\left(0,\frac{b}{2},0\right),\quad \overline{\tau}_{yz}=\frac{h}{q_oa}\tau_{yz}\left(\frac{a}{2},0,0\right)$$

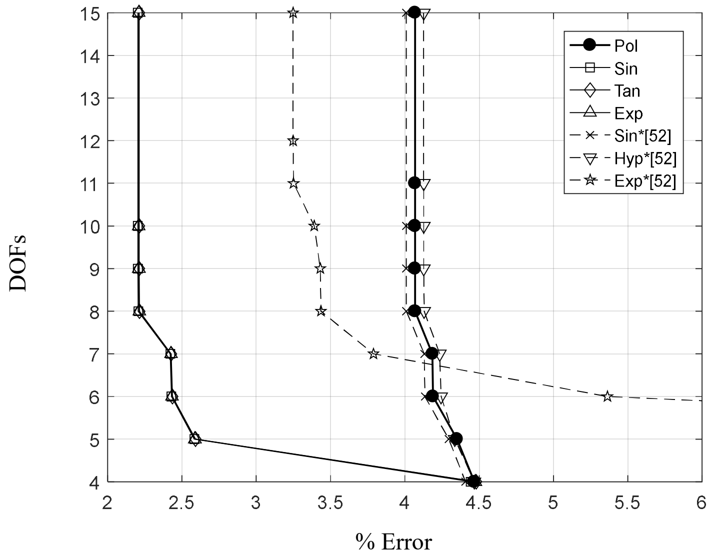

(a) $a/h=4$

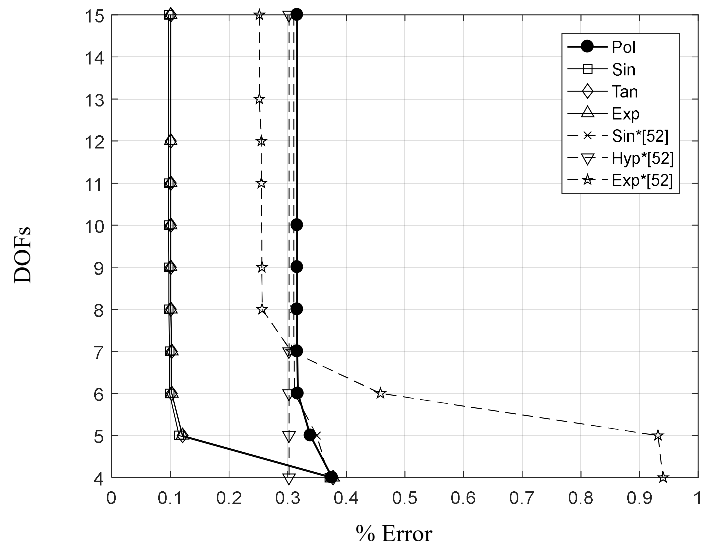

(b) $a/h=20$

Fig. 4. Comparison between BTDs of polynomial and non-polynomial ED4 models build by the AAM for σ_{xz} stress in three layers laminated plate, (a) a/h=4, (b) a/h=20.

The results of the LD4 and the proposed model assessmentfor the three-layer configuration case and the four-layer case have been reported in Tables 4 and 5, and Tables 6 and 7, respectively. LD4 results are in perfect accordance with the 3D exact elasticity results by Pagano [51]. Moreover, from Tables 4-7, it can be seen that the proposed non-polynomials models offer more accurate results than the polynomial full model when compared with the 3D elasticity solution. The three-layer ply configuration normal axial stress $\overline{\sigma}_{xx}$ and the shear stress $\overline{\sigma}_{xz}$ BTDs can be found in Figs. 4 and 5, respectively. Figs. 6 and 7, however, show the BTDs of $\overline{\sigma}_{xx}$ and $\overline{\sigma}_{xz}$ for the four-layer ply configuration case. have Tables 8 and 9 report four reduced models which are build using six unknown variables for each length to thickness ratio and ply configuration. For instance, the best *sin* reduced model with six unknown variables gives an error of 0.096% and 0.033% in $\overline{\sigma}_{xx}$ and $\overline{\sigma}_{xz}$, respectively. This model is presented as follows:

$$\begin{aligned} u_x &= z u_{x2} + \sin\left(\frac{z}{5h}\right) u_{x3} + \sin^3\left(\frac{z}{5h}\right) u_{x5} \\ u_y &= \sin\left(\frac{z}{5h}\right) u_{x3} + \sin^2\left(\frac{z}{5h}\right) u_{x4} \\ u_z &= u_{z1} \end{aligned} \tag{41a-c}$$

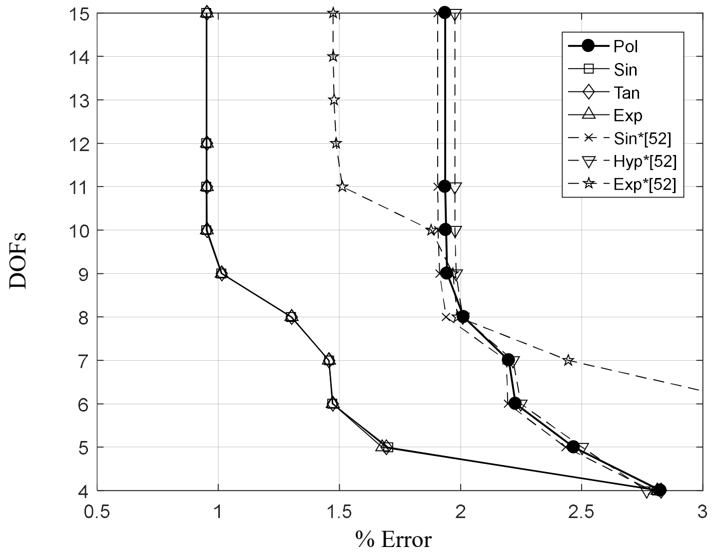

(a) $^a/_h = 4$

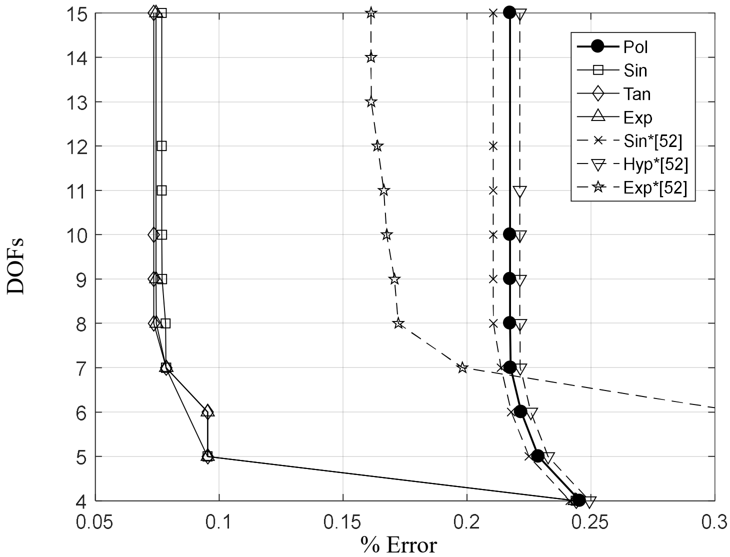

(b) $^a/_h = 20$

Fig. 5. Comparison between BTDs of polynomial and non-polynomial ED4 models build by the AAM for σ_{xx} stress in four layers laminated plate, (a) $^a/_h$=4, (b) $^a/_h$=20.

Figs. 7-10 show the reduced models for axial and shear stress distribution along thickness, respectively. The results suggest that:

- For both studied length to thickness ratios, the reduced models from the new trigonometric and exponential expansions can achieve a better accuracy than polynomial reduced models for a set number of unknown variables.
- For thin plates, all the displacement fields can accurately describe the mechanical behavior of the plate. The reduced models built with only 4 unknown variables can compute errors less than 0.6%.
- All BTDs of new trigonometric and exponential theories presented in this paper are practically the same.
- For the results evaluated, $\overline{\sigma}_{xx}$ and $\overline{\sigma}_{xz}$, u_x terms seem to be more important.
- The *tan* and *exp* best reduced model for 6 unknown variables consists of the same active terms.

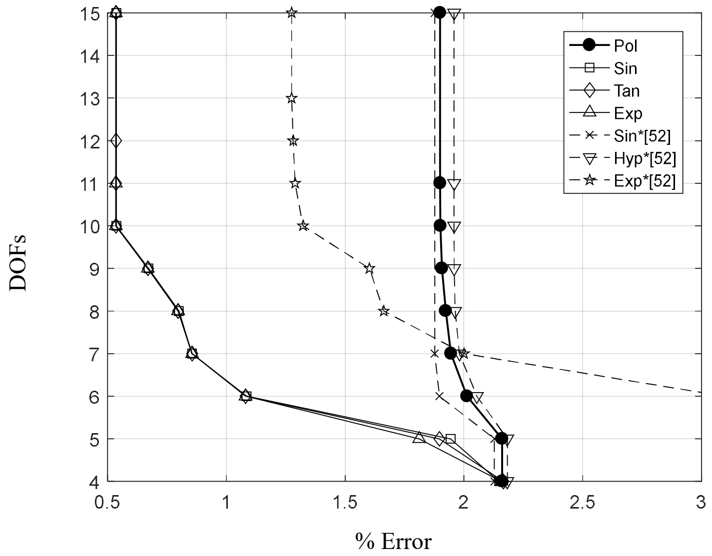

(a) $a/_h = 4$

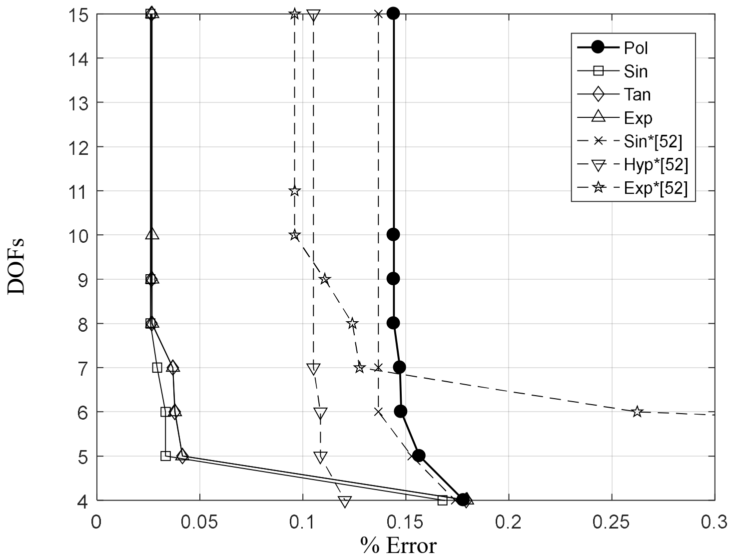

(b) $a/_h = 20$

Fig. 6. Comparison between BTDs of polynomial and non-polynomial ED4 models build by the AAM for σ_{xz} stress in four layers laminated plate, (a) $a/_h$=4, (b) $a/_h$=20.

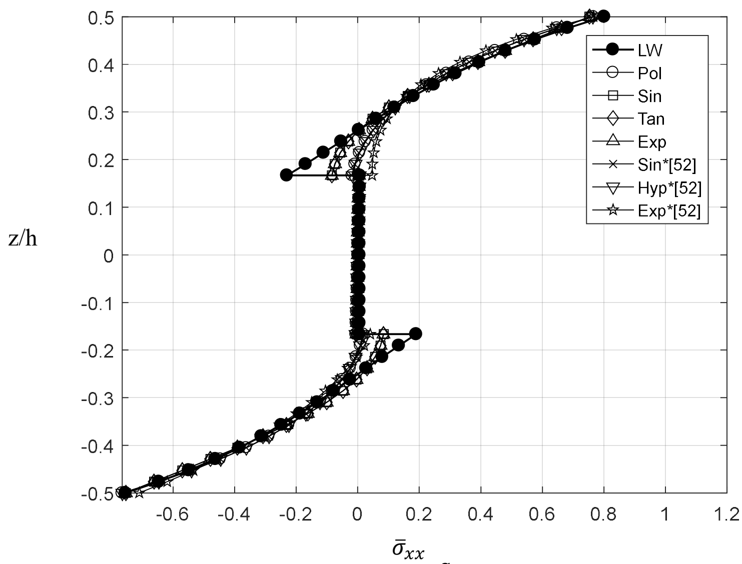

(a) $a/_h = 4$

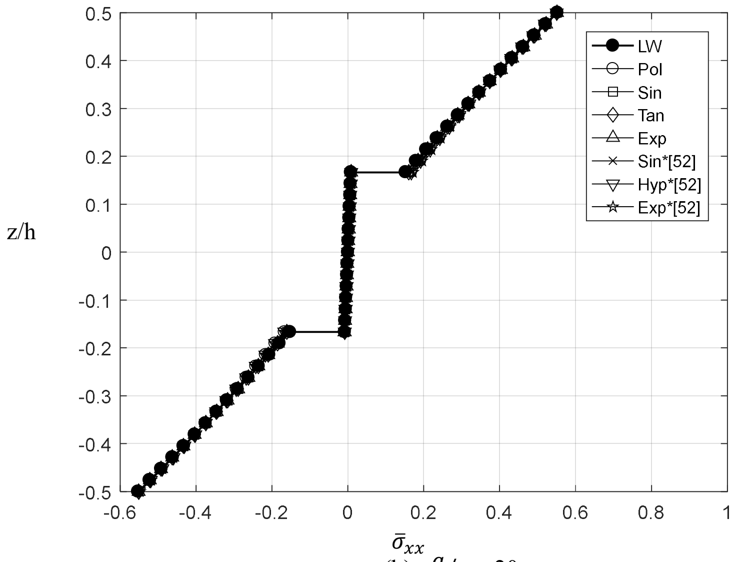

(b) $^{a}/_{h} = 20$

Fig. 7. σ_{xx} distribution along the thickness for the reduced models from Table 8 (a) $^{a}/_{h} = 4$, (b) $^{a}/_{h} = 20$.

Table 4. LD4 model assessment of the proposed theories for three layers symmetric laminated plate, $^{a}/_{h} = 4$.

Ratio 4	w	sxx	syy	sxy	sxz	syz	Average Error
3D Ref. [51]	2.006	-0.755	-0.556	0.051	0.256	0.217	
LW	1.9803	-0.7548	-0.5563	0.0505	0.2559	0.218	0.31%
Pol	1.8663	-0.7402	-0.5070	0.0484	0.279	0.2102	5.67%
Sin	1.8969	-0.7379	-0.5169	0.0487	0.2651	0.2136	3.90%
Tan	1.8967	-0.7379	-0.5168	0.0487	0.2652	0.2136	3.91%
Exp	1.8968	-0.7379	-0.5169	0.0487	0.2652	0.2136	3.91%

Table 5. LD4 model assessment of the proposed theories for three layers symmetric laminated plate, $^{a}/_{h} = 20$.

Ratio 20	$\bar{w}$	$\bar{\sigma}_{xx}$	$\bar{\sigma}_{yy}$	$\bar{\sigma}_{xy}$	$\bar{\sigma}_{xz}$	$\bar{\sigma}_{yz}$	Average Error
LW	0.5163	-0.5525	-0.2101	0.0234	0.3846	0.0938	
Pol	0.5051	-0.5503	-0.2054	0.0231	0.3872	0.0923	1.394%
Sin	0.5101	-0.5514	-0.2074	0.0232	0.3855	0.0929	0.789%
Tan	0.5101	-0.5513	-0.2074	0.0232	0.3856	0.0929	0.796%
Exp	0.5101	-0.5513	-0.2074	0.0232	0.3856	0.0929	0.796%

Table 6. LD4 model assessment of the proposed theories for four layers symmetric laminated plate, $^{a}/_{h} = 4$.

Ratio 4	$\bar{w}$	$\bar{\sigma}_{xx}$	$\bar{\sigma}_{yy}$	$\bar{\sigma}_{xy}$	$\bar{\sigma}_{xz}$	$\bar{\sigma}_{yz}$	Average Error
3D Ref. [51]	1.954	0.720	0.663	-0.047	0.219	0.291	
LW	1.903	0.720	0.663	-0.047	0.219	0.292	0.537%
Pol	1.836	0.722	0.615	-0.046	0.226	0.295	3.440%
Sin	1.859	0.717	0.625	-0.046	0.221	0.290	2.251%
Tan	1.859	0.717	0.625	-0.046	0.221	0.290	2.252%
Exp	1.859	0.717	0.625	-0.046	0.221	0.290	2.252%

Table 7. LD4 model assessment of the proposed theories for four layers symmetric laminated plate, $^{a}/_{h} = 20$.

Ratio 20	$\bar{w}$	$\bar{\sigma}_{xx}$	$\bar{\sigma}_{yy}$	$\bar{\sigma}_{xy}$	$\bar{\sigma}_{xz}$	$\bar{\sigma}_{yz}$	Average Error
LW	2.068	0.587	0.842	0.059	0.144	0.121	
Pol	2.026	0.506	0.823	0.059	0.135	0.119	4.378%
Sin	2.048	0.541	0.831	0.059	0.136	0.120	2.779%
Tan	2.048	0.541	0.831	0.059	0.136	0.120	2.831%
Exp	2.048	0.541	0.831	0.059	0.136	0.120	2.828%

Table 8. ED4 reduced models with 6 unknown variables for $\bar{\sigma}_{xx}$ and $\bar{\sigma}_{xz}$ forthree layers symmetric laminated plate.

		pol	sin	tan	exp	M_E
		a/h = 4				
		Δ ▲ Δ ▲ Δ	Δ ▲ ▲ Δ ▲	Δ ▲ ▲ Δ ▲	Δ ▲ ▲ Δ ▲	
		Δ ▲ Δ ▲ Δ	Δ ▲ Δ Δ Δ	Δ Δ ▲ Δ Δ	Δ Δ ▲ Δ Δ	6/15
		▲ Δ Δ Δ ▲	▲ Δ Δ ▲ Δ	▲ Δ Δ ▲ Δ	▲ Δ Δ ▲ Δ	
Error	σ_{xx}	4.3544 %	2.6339 %	2.6398 %	2.6306 %	
	σ_{xz}	4.5294 %	1.8353 %	1.8506 %	1.8523 %	
		a/h = 20				
		▲ ▲ Δ ▲ Δ	Δ ▲ Δ Δ ▲	Δ ▲ ▲ Δ ▲	Δ ▲ ▲ Δ ▲	
		Δ ▲ Δ Δ Δ	Δ ▲ ▲ Δ Δ	Δ ▲ Δ Δ Δ	Δ ▲ Δ Δ Δ	6/15
		▲ ▲ Δ Δ Δ	▲ Δ Δ ▲ Δ	▲ Δ Δ ▲ Δ	▲ Δ Δ ▲ Δ	
Error	σ_{xx}	0.5847 %	0.2114 %	0.2131 %	0.2129 %	
	σ_{xz}	0.3748 %	0.0986 %	0.1024 %	0.1023 %	

Table 9. ED4 reduced models with 6 unknown variables for $\bar{\sigma}_{xx}$ and $\bar{\sigma}_{xz}$ for four layers symmetric laminated plate.

		pol	sin	tan	exp	M_E
		a/h = 4				
		▲ ▲ Δ ▲ Δ	Δ ▲ ▲ Δ ▲	Δ ▲ ▲ Δ ▲	Δ ▲ ▲ Δ ▲	
		Δ ▲ Δ Δ Δ	Δ ▲ ▲ Δ Δ	Δ ▲ Δ Δ ▲	Δ ▲ Δ Δ ▲	6/15
		▲ ▲ Δ Δ Δ	▲ Δ Δ Δ Δ	▲ Δ Δ Δ Δ	▲ Δ Δ Δ Δ	
Error	σ_{xx}	2.5174 %	1.4708 %	1.4728 %	1.4723 %	
	σ_{xz}	2.0131 %	1.0849 %	1.0808 %	1.0806 %	
		a/h = 20				
		Δ ▲ Δ ▲ Δ	Δ ▲ ▲ Δ ▲	Δ ▲ ▲ Δ ▲	Δ ▲ ▲ Δ ▲	
		Δ ▲ Δ Δ Δ	Δ Δ ▲ ▲ Δ	Δ Δ ▲ Δ Δ	▲ ▲ Δ Δ Δ	6/15
		▲ ▲ ▲ Δ Δ	▲ Δ Δ Δ Δ	▲ Δ Δ ▲ Δ	▲ Δ Δ Δ Δ	
Error	σ_{xx}	0.2364 %	0.0968 %	0.0955 %	0.0953 %	
	σ_{xz}	0.1477 %	0.0334 %	0.0410 %	0.0415 %	

From the stress distribution along thickness, it can be noticed that the reduced models built using non-polynomial terms can reproduce the reference solution stress distribution more accurately. On the other hand, the polynomial reduced model reports problems detecting the mechanical behavior of the plate in regions close to the interlayer.

4.2 Asymmetric laminated plates

A two-layer [0°/90°] cross-ply square plate was considered for the analysis. The normalization used for model assessment was computed via the following equations:

$$\bar{w} = \frac{100E_2h^3}{q_oa^4} w_o\left(\frac{a}{2},\frac{b}{2},\frac{h}{2}\right),\quad \bar{\sigma}_{xx} = \frac{h^2}{q_oa^2}\sigma_{xx}\left(\frac{a}{2},\frac{b}{2},0\right),$$
$$\bar{\sigma}_{yy} = \frac{h^2}{q_oa^2}\sigma_{yy}\left(\frac{a}{2},\frac{b}{2},\frac{h}{2}\right),\quad \bar{\tau}_{xy} = \frac{h^2}{q_oa^2}\tau_{xy}\left(0,0,\frac{-h}{2}\right), \tag{42a-f}$$
$$\bar{\tau}_{xz} = \frac{h}{q_oa}\tau_{xz}\left(0,\frac{b}{2},0\right),\quad \bar{\tau}_{yz} = \frac{h}{q_oa}\tau_{yz}\left(\frac{a}{2},0,0\right)$$

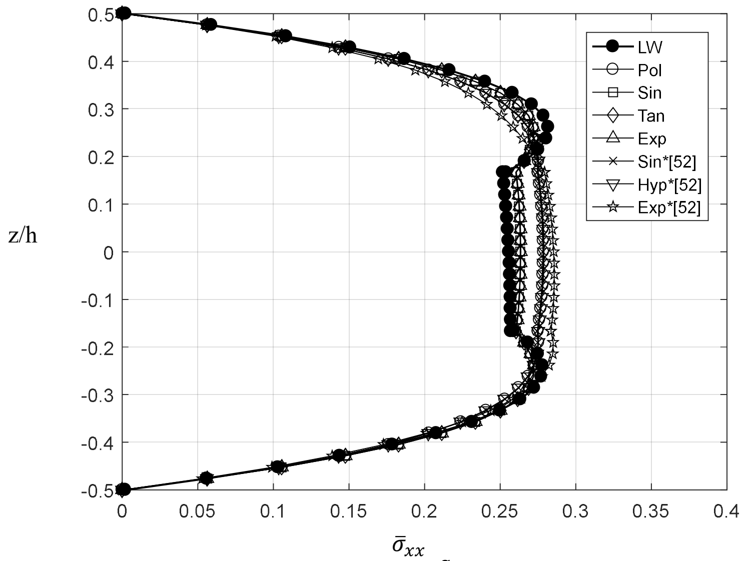

(a) $a/h = 4$

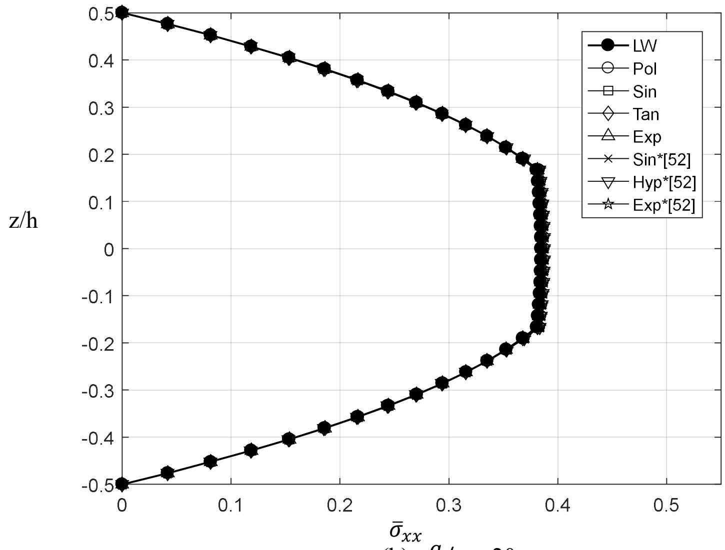

(b) $^{a}/_{h} = 20$

Fig. 8. σ_{xz} distribution along the thickness for the reduced models from Table 8 (a) $^{a}/_{h} = 4$, (b) $^{a}/_{h} = 20$.

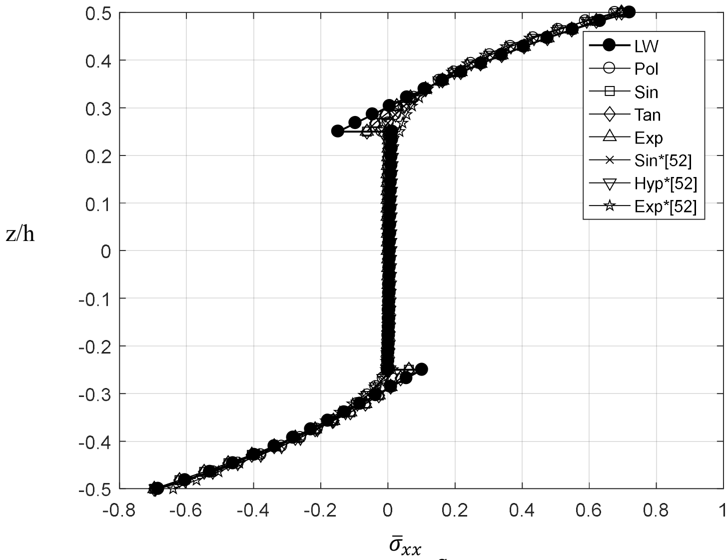

(a) $^{a}/_{h} = 4$

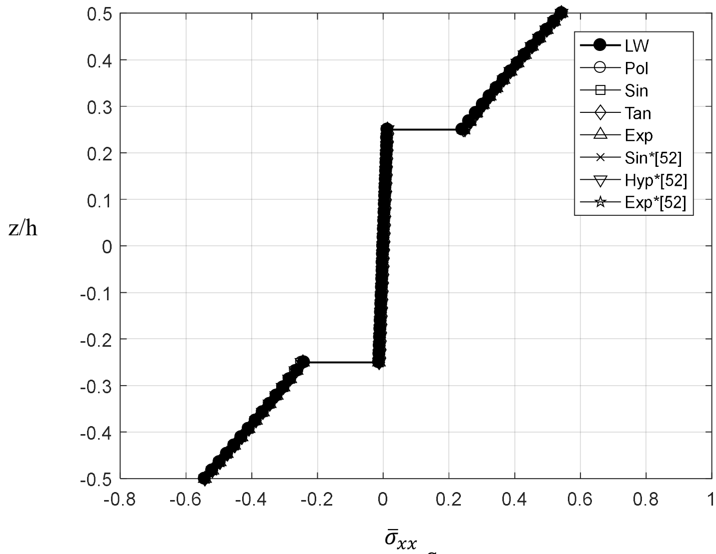

(b) $^{a}/_{h} = 20$

Fig. 9. σ_{xx} distribution along the thickness for the reduced models from Table 9 (a) $^{a}/_{h} = 4$, (b) $^{a}/_{h} = 20$.

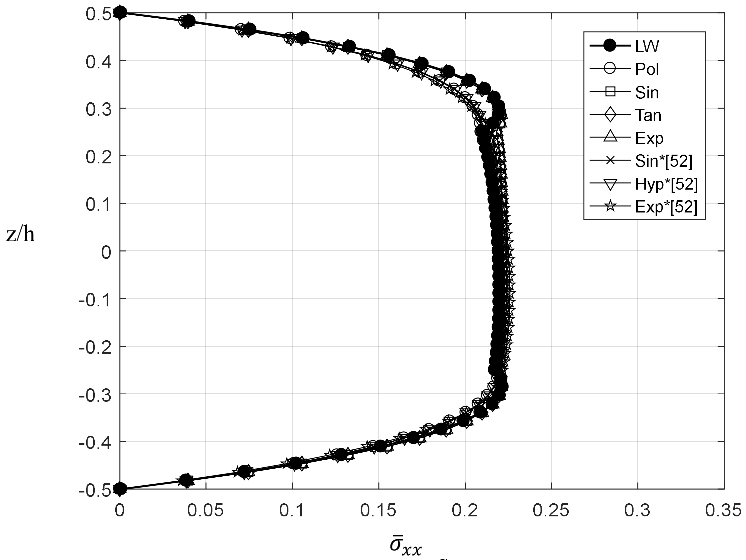

(a) $^a/_h = 4$

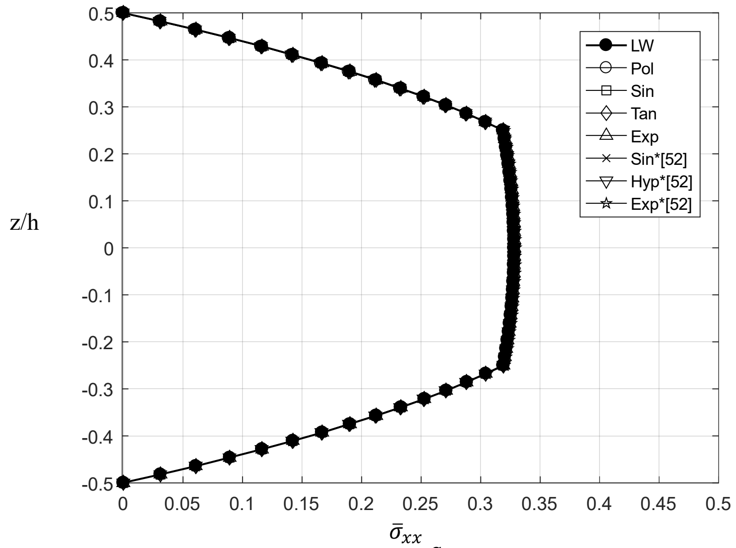

(b) $^a/_h = 20$

Fig. 10. σ_{xz} distribution along the thickness for the reduced models from Table 9 (a) $^a/_h = 4$, (b) $^a/_h = 20$.

Table 10. LD4 model assessment of the proposed theories for two layers asymmetric laminated plate, $^a/_h = 4$.

Ratio 4	$\bar{w}$	$\bar{\sigma}_{xx}$	$\bar{\sigma}_{yy}$	$\bar{\sigma}_{xy}$	$\bar{\sigma}_{xz}$	$\bar{\sigma}_{yz}$	Average Error
LW	2.068	0.587	0.842	0.059	0.144	0.121	
Pol	2.026	0.506	0.823	0.059	0.135	0.119	4.378%
Sin	2.048	0.541	0.831	0.059	0.136	0.120	2.779%
Tan	2.048	0.541	0.831	0.059	0.136	0.120	2.831%
Exp	2.048	0.541	0.831	0.059	0.136	0.120	2.828%

Table 11. LD4 model assessment of the proposed theories for two layers asymmetric laminated plate, $^a/_h = 20$.

Ratio 20	$\bar{w}$	$\bar{\sigma}_{xx}$	$\bar{\sigma}_{yy}$	$\bar{\sigma}_{xy}$	$\bar{\sigma}_{xz}$	$\bar{\sigma}_{yz}$	Average Error
LW	1.105	0.612	0.719	0.053	0.123	0.122	
Pol	1.105	0.612	0.719	0.053	0.123	0.122	0.204%
Sin	1.104	0.611	0.719	0.053	0.123	0.122	0.155%
Tan	1.104	0.611	0.719	0.053	0.123	0.122	0.158%
Exp	1.104	0.611	0.719	0.053	0.123	0.122	0.158%

The LD4 and the proposed assessment models can be found in Tables 10 and 11 for three and four layers, respectively. Similar to the symmetric case, non-polynomial ED4 models presented closer results to the reference solution than the polynomial model whose results exhibited a high error value. On the other hand, the assessment of thin plates presented excellent values for all models.

Fig. 11 shows BTDs for $\overline{\sigma}_{xx}$, whereas BTDs for $\overline{\sigma}_{xz}$ can be found in Fig. 12. The reduced models for thin and thick plates can be found in Table 12 with their respective through-the- thickness distributions presented in Figs. 13 and 14. From the results, the following remarks can be outlined:

- From the BTDs and reported reduced models, it can be seen that non-polynomial reduced models lead to more accurate results evaluating $\bar{\sigma}_{xx}$ and $\overline{\sigma}_{xz}$; however, asymmetric plates present higher complexity. Therefore, in order to achieve accurate results, the reduced models require a higher number of unknown variables compared to the symmetric plate case.
- The reduced models can reproduce the stress distribution accurately in regard to the reference solution.
- Similar to the symmetric plate case, the reduced models present more terms along the u_x expansion and the *tan* and *exp* reduced models consist of the same active terms.
- The effectiveness of terms cannot be easily predicted. While the models can achieve good responses for different ratios, the best reduced model usually consists of different terms.

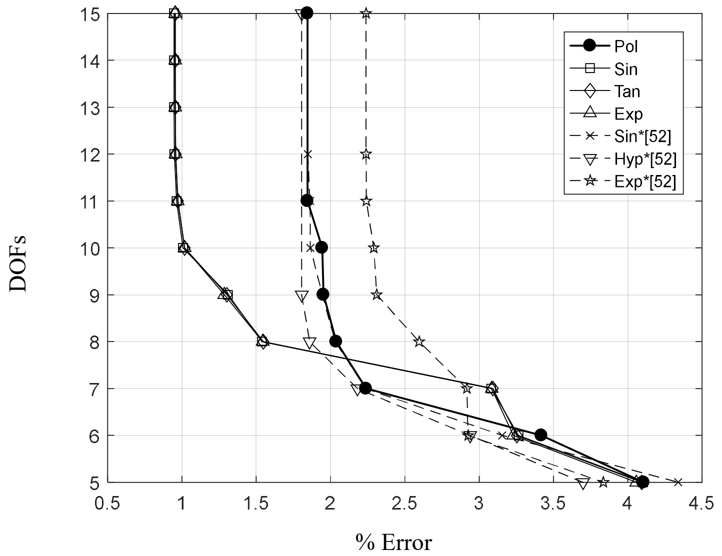

(a) $^{a}/_{h} = 4$

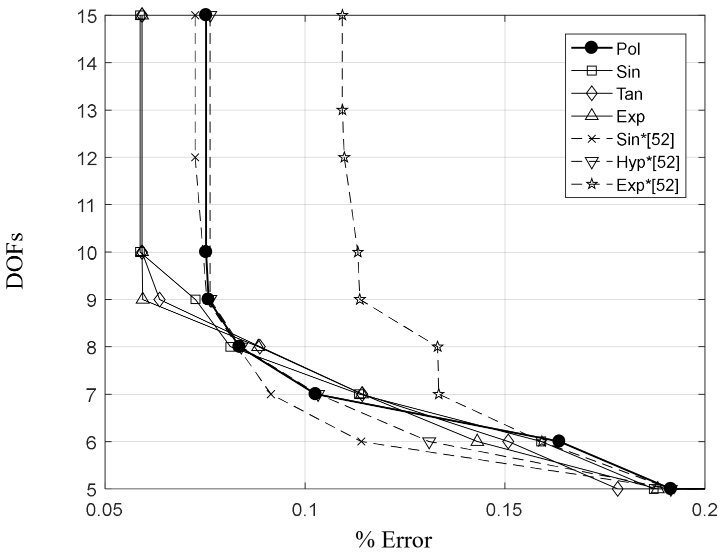

(b) $^{a}/_{h} = 20$

Fig. 11. Comparison between BTDs of polynomial and non-polynomial ED4 models build by the AAM for σ_{xx} stress in two layers laminated plate, (a) $^{a}/_{h}$=4, (b) $^{a}/_{h}$=20.

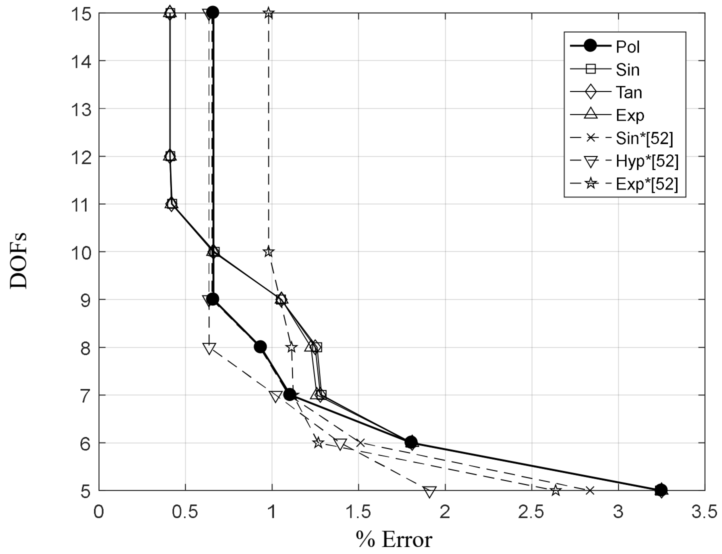

(a) $a/h = 4$

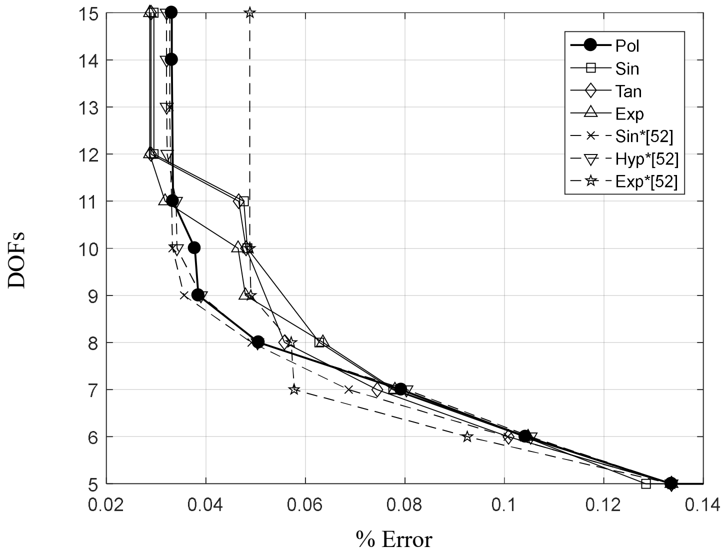

(b) $a/h = 20$

Fig. 12. Comparison between BTDs of polynomial and non-polynomial ED4 models build by the AAM for σ_{xz} stress in two layers laminated plate, (a) a/h=4, (b) a/h=20.

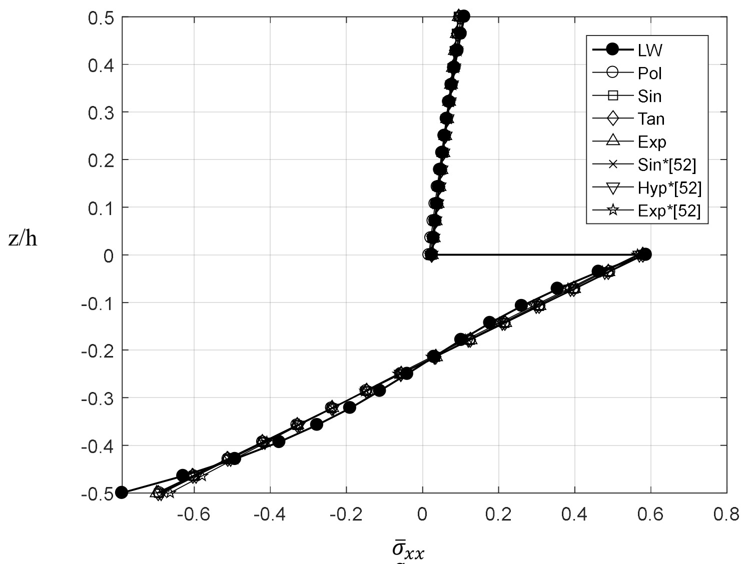

(a) $a/h = 4$

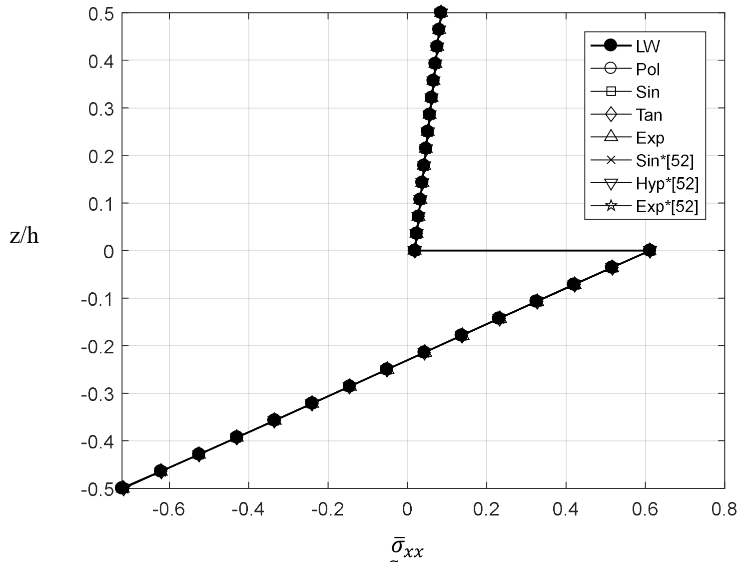

(b) $^{a}/_{h}$ = 20

Fig. 13. σ_{xx} distribution along the thickness for the reduced models from Table 12 (a) $^{a}/_{h}$ = 4, (b) $^{a}/_{h}$ = 20.

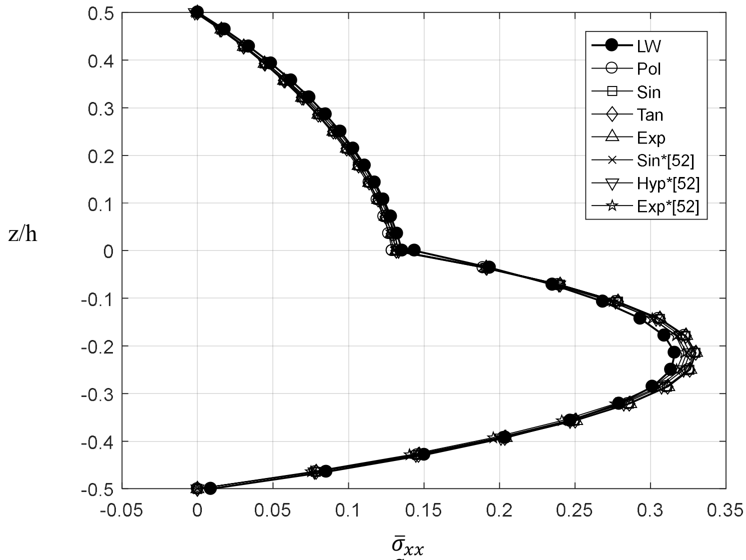

(a) $^{a}/_{h}$ = 4

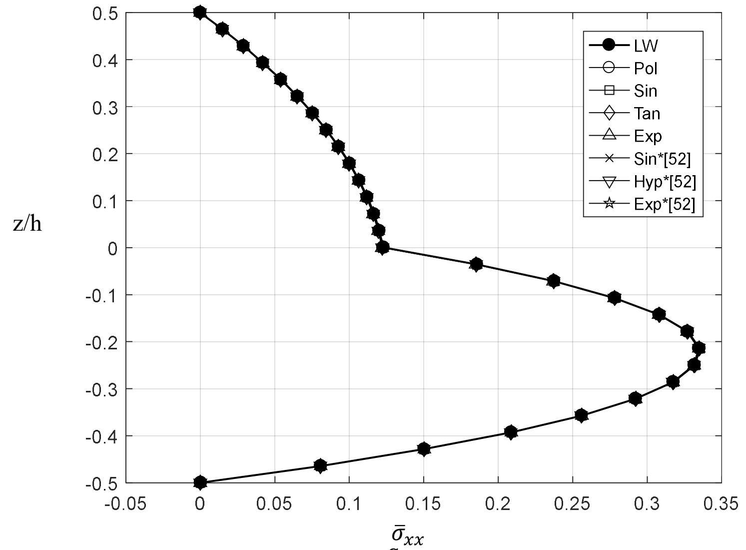

(b) $^{a}/_{h}$ = 20

Fig. 14. σ_{xz} distribution along the thickness for the reduced models from Table 12 (a) $^{a}/_{h}$ = 4, (b) $^{a}/_{h}$ = 20.

Table 12. ED4 reduced models with 6 unknown variables for $\bar{\sigma}_{xx}$ and $\bar{\sigma}_{xz}$ for two layers asymmetric laminated plate.

		pol	sin	tan	exp	M_E
				a/h = 4		
		▲ ▲ Δ Δ Δ	▲ ▲ Δ Δ Δ	▲ Δ ▲ Δ Δ	▲ Δ ▲ Δ Δ	
		▲ ▲ Δ Δ Δ	▲ Δ ▲ Δ Δ	▲ ▲ Δ Δ Δ	▲ ▲ Δ Δ Δ	6/15
		▲ Δ Δ ▲ Δ	▲ Δ ▲ Δ Δ	▲ Δ ▲ Δ Δ	▲ Δ ▲ Δ Δ	
Error	σ_{xx}	3.4191 %	3.2653 %	3.2642 %	3.2307 %	
	σ_{xz}	1.8064 %	1.8837 %	1.8893 %	1.9001 %	
				a/h = 20		
		▲ ▲ Δ Δ Δ	▲ ▲ Δ Δ Δ	▲ Δ ▲ ▲ Δ	▲ Δ ▲ ▲ Δ	
		▲ ▲ Δ Δ Δ	▲ Δ ▲ Δ Δ	▲ ▲ Δ Δ Δ	▲ ▲ Δ Δ Δ	6/15
		▲ ▲ Δ Δ Δ	▲ ▲ Δ Δ Δ	▲ Δ Δ Δ Δ	▲ Δ Δ Δ Δ	
Error	σ_{xx}	0.1636 %	0.1591 %	0.1599 %	0.1431 %	
	σ_{xz}	0.1124 %	0.1068 %	0.1009 %	0.1246 %	

5. Conclusions

The effectiveness of non-polynomial theories in the study of laminated plates was investigated in this paper. The axiomatic/asymptotic method was employed to build reduced models for symmetric and asymmetric cross-ply laminated simply-supported square plates. Errors from ESL reduced models were compared against an LW full theory whose values were in excellent agreement with 3D results.The best reduced models were used to construct the Best Theory Diagram considering different geometries (e.g. length-to-thickness ratio) and ply sequence configurations. The studied cases were analyzed by means of the CUF and the Navier-type closed form solution was obtained. The following main conclusions can be drawn:

- For all thickness ratios, non-polynomial displacement fields offer a more accurate description of the mechanical behavior of the laminated plate including the complete and reduced models.
- The relevance of a displacement term is heavily problem-dependent. The AAM can give insight of the importance of each variable by evaluating the reduced model's accuracy against a reference solution.
- Asymmetric plates reduced models require more unknown variables than symmetric plates to offer acceptable solutions.
- Thin plates reduced models offer very good results and often reduced models derived from the AAM include more terms along the u_x expansion when evaluating axial stress $\bar{\sigma}_{xx}$ and shear stress $\bar{\sigma}_{xz}$.
- While polynomial reduced models have problems detecting the mechanical behavior of the plate in regions close to the interlayer, non polynomial reduced models' stress distributions are closer to the reference solution.

Future works should deal with developing best theory diagrams for a total set of displacements and stresses in multifield problems.

Acknowledgment

This paper was written in the context of the project: "Estudio comparativo del potencial de fibras naturales endémicas del perú para su uso como refuerzo en materiales compuestos laminados" founded by the Consejo Nacional de Ciencia, Tecnología e Innovación Tecnológica (CONCYTEC) under the contrat number N° 117-2016-FONDECYT. The authors of this paper apreciate the financial support from the Peruvian Goverment.

References

[1] Kirchoff, G., Uber das Gleichgewicht und die Bewegung einer elastischen Scheibe, *Journal fur die Reine und Angewandte Mathematik*, 40, 1850, 51-88.

[2] Love, A. E. H., *A treatise on the mathematical theory of elasticity*, Cambridge university press, 2013

[3] Reissner, E., The effect of transverse shear deformation on the bending of elastic plates, *Journal of Applied Mechanics*, 12, 1945, 69-77.

[4] Mindlin, R. D., Influence of rotatory inertia and shear on flexural motions of isotropic, elastic plates, *Journal of Applied Mechanics*, 18, 1031-1036.

[5] Vlasov, B. F., *On the equations of bending of plates*, Dokla Ak Nauk Azerbeijanskoi-SSR, 3, 1957, 955-979.

[6] Jemielita, G., *Technical theory of plates with moderate thickness*, Rozprawy Ink, 23(3), 1975, 483-499.

[7] Schmidt, R., A refined nonlinear theory of plates with transverse shear deformation, *Journal of Industrial Mathematics Society*, 27(1), 1977, 23-38.

[8] Reddy, J. N., A general non-linear third-order theory of plates with moderate thickness, *International Journal of Non-Linear Mechanics*, 25(6), 1990, 677-686.

[9] Levy M., Mémoire sur la théorie des plaques élastiques planes, *Journal de Mathématiques Pures et Appliquées*, 30, 1877, 219-306

[10] Stein M., Nonlinear theory for plates and shells including the effects of transverse shearing, *AIAA Journal*, 24(9), 1986, 1537-1544.

[11] Shimpi, R. P., Ghugal, Y. M., A new layerwise trigonometric shear deformation theory for two-layered cross-ply beams, *Composites Science and Technology*, 61(9), 2001, 1271-1283.

[12] Touratier M., An efficient standard plate theory, *International Journal of Engineering Science*, 29(8), 1991, 901-916.

[13] Soldatos K., A transverse shear deformation theory for homogeneous monoclinic plates, *Acta Mechanica*, 94(3), 1992, 195-220.

[14] Ferreira, A. J. M., Roque, C. M. C., Jorge, R. M. N., Analysis of composite plates by trigonometric shear deformation theory and multiquadrics, *Computers & Structures*, 83(27), 2005, 2225-2237.
[15] Karama, M., Afaq, K. S., Mistou, S., A new theory for laminated composite plates, *Proceedings of the Institution of Mechanical Engineers, Part L: Journal of Materials: Design and Applications*, 223(2), 2009, 53-62.
[16] Akavci S., Two new hyperbolic shear displacement models for orthotropic laminated composite plates, *Mechanics of Composite Materials*, 46(2), 2010, 215-226.
[17] Mantari, J. L., Oktem, A. S., Soares, C. G., A new trigonometric shear deformation theory for isotropic, laminated composite and sandwich plates *International Journal of Solids and Structures*, 49(1), 2012, 43-53.
[18] Mantari, J. L., Soares, C. G., Analysis of isotropic and multilayered plates and shells by using a generalized higher-order shear deformation theory, *Composite Structures*, 98(8), 2012, 2640-2656.
[19] Thai, C. H., Ferreira, A. J. M., Bordas, S. P. A., Rabczuk, T., Nguyen-Xuan, H., Isogeometric analysis of laminated composite and sandwich plates using a new inverse trigonometric shear deformation theory, *European Journal of Mechanics-A/Solids*, 43, 2014, 89-108.
[20] Zenkour, A. M., Thermal bending of layered composite plates resting on elastic foundations using four-unknown shear and normal deformations theory, *Composite Structures*, 122, 2015, 260-270.
[21] Grover, N., Maiti, D. K., Singh, B. N., A new inverse hyperbolic shear deformation theory for static and buckling analysis of laminated composite and sandwich plates, *Composite Structures*, 95, 2013, 667-675.
[22] Sarangan, S., Singh, B. N., Higher-order closed-form solution for the analysis of laminated composite and sandwich plates based on new shear deformation theories, *Composite Structures*, 138, 2016, 391-403.
[23] Mahi, A., Tounsi, A., A new hyperbolic shear deformation theory for bending and free vibration analysis of isotropic, functionally graded, sandwich and laminated composite plates, *Applied Mathematical Modelling*, 39(9), 2015, 2489-2508.
[24] Carrera, E., *A class of two-dimensional theories for anisotropic multilayered plates analysis*, Atti della accademia delle scienze di Torino. Classe di scienze fisiche matematiche e naturali, 19, 1995, 1-39.
[25] Carrera, E., Theories and finite elements for multilayered plates and shells: a unified compact formulation with numerical assessment and benchmarking, *Archives of Computational Methods in Engineering*, 10(3), 2003, 215-296.
[26] Carrera, E., Giunta, G., Petrolo, M., *Beam structures: classical and advanced theories*, John Wiley & Sons, 2011.
[27] Carrera, E., Cinefra, M., Petrolo, M., Zappino, E., *Finite element analysis of structures through unified formulation*, John Wiley & Sons, 2014.
[28] Carrera, E., Petrolo, M., Guidelines and recommendations to construct theories for metallic and composite plates, *AIAA Journal*, 48(12), 2010, 2852-2866.
[29] Carrera, E., Petrolo, M., On the effectiveness of higher-order terms in refined beam theories, *Journal of Applied Mechanics*, 78(2), 2011, 1-17.
[30] Carrera, E., Miglioretti, F., Petrolo, M., Guidelines and recommendations on the use of higher order finite elements for bending analysis of plates, *International Journal for Computational Methods in Engineering Science and Mechanics*, 12(6), 2011, 303-324.
[31] Carrera, E., Miglioretti, F., Petrolo, M., Accuracy of refined finite elements for laminated plate analysis, *Composite Structures*, 93(5), 2011, 1311-1327.
[32] Carrera, E., Miglioretti, F., Petrolo, M., Computations and evaluations of higher-order theories for free vibration analysis of beams, *Journal of Sound and Vibration*, 331(19), 2012, 4269-4284.
[33] Carrera, E., Miglioretti, F., Selection of appropriate multilayered plate theories by using a genetic like algorithm, *Composite Structures*, 94(3), 2012, 1175-1186.
[34] Mashat, D. S., Carrera, E., Zenkour, A. M., Al Khateeb, S. A., Use of axiomatic/asymptotic approach to evaluate various refined theories for sandwich shells, *Composite Structures*, 109, 2014, 139-149.
[35] Mashat, D. S., Carrera, E., Zenkour, A. M., Al Khateeb, S. A., Axiomatic/asymptotic evaluation of multilayered plate theories by using single and multi-points error criteria, *Composite Structures*, 106, 2013, 393-406.
[36] Mashat, D. S., Carrera, E., Zenkour, A. M., Al Khateeb, S. A., Lamberti, A., Evaluation of refined theories for multilayered shells via Axiomatic/Asymptotic method, *Journal of Mechanical Science and Technology*, 28(11), 2014, 4663-4672.
[37] Cinefra, M., Lamberti, A., Zenkour, A. M., Carrera, E., Axiomatic/asymptotic technique applied to refined theories for piezoelectric plates, *Mechanics of Advanced Materials and Structures*, 22(1-2), 2015, 107-124.
[38] Carrera, E., Cinefra, M., Lamberti, A., Zenkour, A. M., Axiomatic/asymptotic evaluation of refined plate models for thermomechanical analysis, *Journal of Thermal Stresses*, 38(2), 2015, 165-187.
[39] Carrera, E., Cinefra, M., Lamberti, A., Petrolo, M., Results on best theories for metallic and laminated shells including Layer-Wise models, *Composite Structures*, 126, 2015, 285-298.
[40] Petrolo, M., Cinefra, M., Lamberti, A., Carrera, E., Evaluation of mixed theories for laminated plates through the axiomatic/asymptotic method, *Composites part B: Engineering*, 76, 2015, 260-272.
[41] Petrolo, M., & Lamberti, A., Axiomatic/asymptotic analysis of refined layer-wise theories for composite and sandwich plates, *Mechanics of Advanced Materials and Structures*, 23(1), 2016, 28-42.
[42] Petrolo, M., Lamberti, A., Miglioretti, F., Best theory diagram for metallic and laminated composite plates, *Mechanics of Advanced Materials and Structures*, 23(9), 2016, 1114-1130.
[43] Cinefra, M., Carrera, E., Lamberti, A., Petrolo, M., Best theory diagrams for multilayered plates considering multifield analysis, *Journal of Intelligent Material Systems and Structures*, 28(16), 2017, 2184-2205.
[44] Neves, A. M. A., Ferreira, A. J. M., Carrera, E., Cinefra, M., Jorge, R. M. N., Soares, C. M. M., Buckling analysis of sandwich plates with functionally graded skins using a new quasi-3D hyperbolic sine shear deformation theory and collocation with radial basis functions, *ZAMM-Zeitschrift fur Angewandte Mathematikund Mechanik*, 92(9), 2012, 749-766.

[45] Carrera, E., Filippi, M., Zappino, E., Laminated beam analysis by polynomial, trigonometric, exponential and zig-zag theories, *European Journal of Mechanics-A/Solids*, 41, 2013, 58-69.

[46] Carrera, E., Filippi, M., & Zappino, E., Free vibration analysis of laminated beam by polynomial, trigonometric, exponential and zig-zag theories, *Journal of Composite Materials*, 48(19), 2014, 2299-2316.

[47] Filippi, M., Carrera, E., Zenkour, A. M., Static analyses of FGM beams by various theories and finite elements, *Composites Part B: Engineering*, 72, 2015, 1-9.

[48] Filippi, M., Petrolo, M., Valvano, S., Carrera, E., Analysis of laminated composites and sandwich structures by trigonometric, exponential and miscellaneous polynomials and a MITC9 plate element, *Composite Structures*, 150, 2016, 103-114.

[49] Mantari, J. L., Ramos, I. A., Carrera, E., Petrolo, M., Static analysis of functionally graded plates using new non-polynomial displacement fields via Carrera Unified Formulation, *Composites Part B: Engineering*, 89, 2016, 127-142.

[50] Ramos, I. A., Mantari, J. L., Zenkour, A. M., Laminated composite plates subject to thermal load using trigonometrical theory based on Carrera Unified Formulation, *Composite Structures*, 143, 2016, 324-335.

[51] Pagano, N. J., Exact solutions for rectangular bidirectional composites and sandwich plates, *Journal of Composite Materials*, 4(1), 1970, 20-34.

[52] Candiotti, S., Mantari, J. L., Yarasca, J., Petrolo, M., Carrera, E., An axiomatic/asymptotic evaluation of best theories for isotropic metallic and functionally graded plates employing non-polynomic functions, *Aerospace Science and Technology*, 68, 2017, 179-192.